Phosphonium Ylides vs Iminophosphoranes: The Role of the Coordinating Ylidic Atom in cis -[Phosphine-Ylide Rh(CO) 2] Complexes

Ingrid Popovici, Thibault Tannoux, Cécile Barthes, Carine Duhayon, Nicolas Casaretto, Antonio Monari, Audrey Auffrant, Yves Canac

Phosphonium Ylides vs Iminophosphoranes: The Role of the Coordinating Ylidic Atom in *cis*-[Phosphine-Ylide $Rh(CO)_2$] Complexes

Ingrid Popovici,[b] Cécile Barthes,[a] Thibault Tannoux,[b] Carine Duhayon,[a] Nicolas Casaretto,[b] Antonio Monari,[c]* Audrey Auffrant,[b]* Yves Canac[a]*

a) LCC-CNRS, Université de Toulouse, CNRS, 205 route de Narbonne, 31077 Toulouse Cedex 4, France.
b) Laboratoire de Chimie Moléculaire (LCM), CNRS, École Polytechnique, Institut Polytechnique de Paris, Route de Saclay, 91120 Palaiseau, France.
c) Université Paris Cité and CNRS, ITODYS, F-75006, Paris, France.

ABSTRACT:
The coordinating properties of two families of ylides, namely phosphonium ylides and iminophosphoranes, differently substituted at the ylidic center (CH_2^- vs N*i*Pr$^-$), have been investigated in structurally related cationic phosphine-ylide $Rh(CO)_2$ complexes obtained from readily available phosphine-phosphonium salt precursors derived from an *ortho*-phenylene bridge. However, while the $Rh(CO)_2$ complex bearing the P^+–CH_2^- donor moiety proved to be stable, the P=N*i*Pr donor end appeared to induce lability to one of the CO groups. All the Rh^I carbonyl complexes in both ylide series were fully characterized, including through X-ray diffraction analysis. Based on the experimental and calculated infrared (IR) CO stretching frequencies in $Rh(CO)_2$ complexes, we evidenced that the phosphonium ylide ligand is a stronger donor than the iminophosphorane ligand. However, we also found that the difference in the intrinsic electronic properties can be largely compensated by the introduction of an *i*Pr substituent on the N atom of the iminophosphorane, hence pointing to the non-innocent role of the peripheral substituent and opening novel possibilities to tune the properties of metal complexes containing ylide ligands.

Keywords: Iminophosphorane, Phosphonium ylide, Chelating ligand, Electron-donation, Infrared (IR) CO stretching frequency, Rhodium complex.

INTRODUCTION

Phosphonium ylides, discovered a long time ago following the successive work of Michaelis,[1] Staudinger, and Meyer,[2] are best known for their essential role in organic synthesis, mainly in Wittig-type reactions for the selective formation of C=C bonds.[3] The substitution of the negatively charged C-sp^3 hybridized carbon atom, which is stabilized by the nearby tetrahedral phosphonium, by an anionic N-sp^2 hybridized atom results in the formation of another well-known family of phosphorus derivatives, namely the iminophosphoranes (also called phosphinimines or phosphazenes). The latter species, initially reported by the same authors,[2] behave like phosphonium ylides as valuable intermediates in organic chemistry, playing a crucial role in the formation of C=N bonds through the related aza-Wittig reaction.[3] Although several computational studies have been carried out in the past evidencing different electron density organization,[4] the bonding pattern in the isoelectronic phosphonium ylides and iminophosphoranes presents certain analogies. In particular it may be formally described as a strongly polarized P=X bond (X = C or N) involving the resonance between two canonical limiting forms, i.e. the neutral ylene and the ionic ylide (Figure 1).

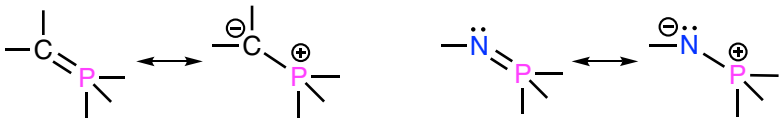

Figure 1. Representation of the two canonical forms of C−P bonding in phosphonium ylides (*left*) and N−P bonding in iminophosphoranes (*right*).

While invoking the ylene form could account for the short P–X bond distance and hence the strong interaction between P and X atoms, it can be misleading in the sense that those units have no available π system and therefore almost no accepting ability. The short P–X bond distance is better explained by both strong ionic interactions and negative hyperconjugation, which stabilize the X electron density via the neighboring electron-deficient phosphorus atom.[5] Despite the lack of systematic comparisons between iminophosphoranes and phosphonium ylides, molecular modeling has pointed towards a slightly higher P–X bond order in PH_3=NH compared to PH_3=CH_2.[6] In the case of phosphonium ylides, the ylidic bond was alternatively described in terms of donor-acceptor interactions between closed-shell R_3P: and :CR_2 fragments with the contribution of two pairs of electrons.[7] Beyond the difference in the electronegativity of the ylidic-type atom (C: 2.5 vs N: 3.0), phosphonium ylides[8] and iminophosphoranes[9] behave mainly as η^1-ligands with strong σ-donor and relatively weak π-acceptor character either in

main group[10] or coordination chemistry.[11] Moreover and especially compared to NHCs,[12] while ylide-based ligands act as harder donors which, *a priori,* should be more prone to coordinate electropositive metals, their overall neutral character allows accommodating late metal elements, similarly to NHCs.[8-9] For catalytic purposes, examples involving P^+–C^- ylide ligands remain scarce, certainly due to synthetic and stability issues of the corresponding metal complexes.[13] However, the pioneering report of a diylide rhodium complex active for olefin hydrogenation is worth mentioning,[14] as well as the more recent study concerning a NHC core palladium pincer exhibiting two side ylide ends for the allylation of aldehydes.[15] For their part, P=N ylides have also proved useful in catalysis such as in oligomerization, polymerization or coupling reactions,[16] but remain, like their carbon analogues, largely underexploited in this field of application. Regarding the electronic properties of ylide ligands, it has been shown both experimentally and theoretically that the donor character of phosphonium ylides is stronger than that of the highly σ-donating NHCs through the preparation of an isostructural series of Rh^I dicarbonyl complexes.[17] The better donor capability of iminophosphoranes with respect to NHCs has also been briefly pointed out,[11j] however no systematic study has been undertaken to directly compare the electronic features of both category of ylides. Based on this, a systematic ranking of the donor ability of these two families of ylides is still highly desirable to obtain a better understanding of the electronic factors that govern the stability vs reactivity of the corresponding metal complexes. For this purpose, we targeted *cis*-[LL'$Rh(CO)_2$] complexes bearing the same global charge and built from a rigid *ortho*-phenylene bridge, where LL' represents a *cis*-chelating ligand featuring a tri(aryl)phosphine end and an ylide donor extremity which can be either a phosphonium ylide (**D-1**) or an iminophosphorane (**D-2**). Furthermore, the coordination mode of LL' ligands together with the square-planar geometry in the targeted five-membered Rh^I metallacycles is expected to be beneficial for the introduction of carbonyl co-ligands acting as experimental infrared (IR) probes. The latter offer an opportunity to evaluate the overall σ-donating vs π-accepting properties of the two ylide ligands of interest (Figure 2).

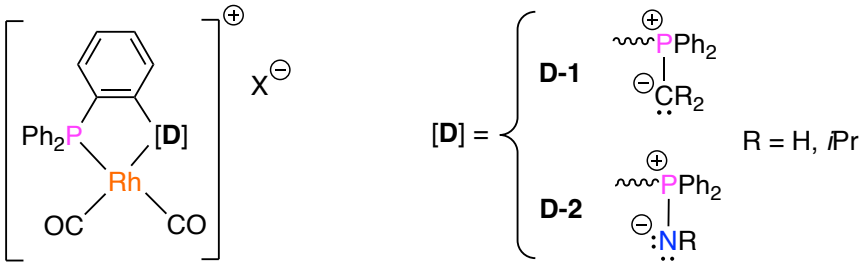

Figure 2. Representation of targeted *cis*-[LL'Rh(CO)$_2$] complexes featuring an *ortho*-phenylene bridge substituted by phosphine and ylide donor extremities.

Thus, the present contribution addresses the preparation, the characterization in solution and solid state, and the molecular modeling of cationic Rh^{I}(CO)$_2$ complexes obtained from readily available chelating phosphine-ylide ligands. This provides a direct comparison of the electronic properties between the two families of ylide ligands, which is not only fundamental in organic synthesis but also brings further interest for organometallic chemistry and homogeneous catalysis.

RESULTS AND DISCUSSION

Synthesis and Spectroscopic Characterization of *cis*-[Phosphine-Phosphonium Ylide Rh^{I}] Complexes.

Our first target was the **[L^{C}Rh(CO)$_2$](OTf)** complex featuring a *cis*-chelating phosphine-phosphonium ylide ligand. For this purpose, *o*-diphenylphosphinobenzene (*o*-dppb) was reacted with one equivalent of methyltriflate in CH_2Cl_2 at –78°C affording selectively the phosphino-phosphonium salt **L^{C}H.OTf** in 98 % yield (Scheme 1, *top*).[18] The structure of **L^{C}H.OTf** was first assigned on the basis of ^{31}P NMR (δ_P = 22.3 ppm (d, P$^+$) and δ_P = –15.4 ppm (d, P), J_{PP} = 25.9 Hz) and ^{1}H NMR spectroscopy (δ_H = 3.10 ppm, dd, J_{PH} = 4.0 and 14.0 Hz, PCH_3). The exact structure of **L^{C}H.OTf** was unambiguously confirmed by X-ray diffraction analysis of colorless single crystals obtained from CH_2Cl_2/pentane at room temperature (Figure 3, *left*).[19] The coordination behavior of the pre-ligand **L^{C}H.OTf** towards a Rh^{I} fragment was then investigated. Deprotonation of the P-methyl substituent of the phosphonium **L^{C}H.OTf** with *n*BuLi followed by the addition of 0.5 equivalent of [Rh(COD)Cl]$_2$ in THF at –78°C readily led to the corresponding chelate phosphine-phosphonium ylide complex **[L^{C}Rh(COD)](OTf)** in 90% yield (Scheme 1, *bottom*). The significant shift of the ^{31}P NMR signals and the observed multiplicity at δ_P = 32.7 ppm (dd, J_{PP} = 25.9 Hz and J_{RhP} = 162.0 Hz, P) and δ_P = 28.6 ppm (dd, J_{PP} = 25.9 Hz and J_{RhP} = 4.8 Hz,

PCH_2) are both in agreement with the expected ylide rhodium complex structure of **[L^{C}Rh(COD)](OTf)**. The presence of the Rh–CH_2 unit was confirmed by multinuclear NMR spectroscopy and, in particular, by the high-field ^{13}C NMR signal and the multiplicity of the metalated ylidic carbon atom (δ_{CH2} = –2.2 ppm, ddd, J_{PC} = 12.1 and 35.2 Hz, J_{RhC} = 24.1 Hz). To obtain some insights into the electronic properties of the chelating phosphine-phosphonium ylide ligand, the displacement of the COD ligand in complex **[L^{C}Rh(COD)](OTf)** by CO was performed next. For this purpose, CO gas was bubbled through a solution of complex **[L^{C}Rh(COD)](OTf)** in CH_2Cl_2 at room temperature (Scheme 1, *bottom*). The formation of the new **[L^{C}Rh(CO)$_2$](OTf)** complex was achieved after 15 min. as indicated by ^{31}P NMR with the appearance of two new doublets of doublets at δ_P = 27.8 ppm (dd, J_{PP} = 41.3 Hz and J_{RhP} = 4.8 Hz, PCH_2) and δ_P = 21.0 ppm (dd, J_{PP} = 41.3 Hz and J_{RhP} = 129.6 Hz, P). The targeted **[L^{C}Rh(CO)$_2$](OTf)** complex was isolated in 88% yield after addition of pentane to prevent it from reacting with the released COD ligand and partially reforming the complex precursor **[L^{C}Rh(COD)](OTf)**. Interestingly, the relative position of the two ^{31}P NMR resonances of **[L^{C}Rh(CO)$_2$](OTf)** were found to be reversed with respect to those of **[L^{C}Rh(COD)](OTf)**. The presence of the CH_2 ylide functionality was confirmed by ^{13}C NMR spectroscopy (δ_{CH2} = –7.2 ppm, ddd, J_{PC} = 12.1 and 38.2 Hz, J_{RhC} = 19.1 Hz). Moreover, the ^{13}C NMR spectrum of **[L^{C}Rh(CO)$_2$](OTf)** shows two classical deshielded CO signals at δ_C = 186.0 ppm (brs) and δ_C = 184.7 ppm (dd, J_{PC} = 15.6 Hz and J_{RhC} = 58.8 Hz). Finally, the IR CO stretching frequencies of **[L^{C}Rh(CO)$_2$](OTf)** in CH_2Cl_2 were measured at 2024 and 2082 cm^{-1}.

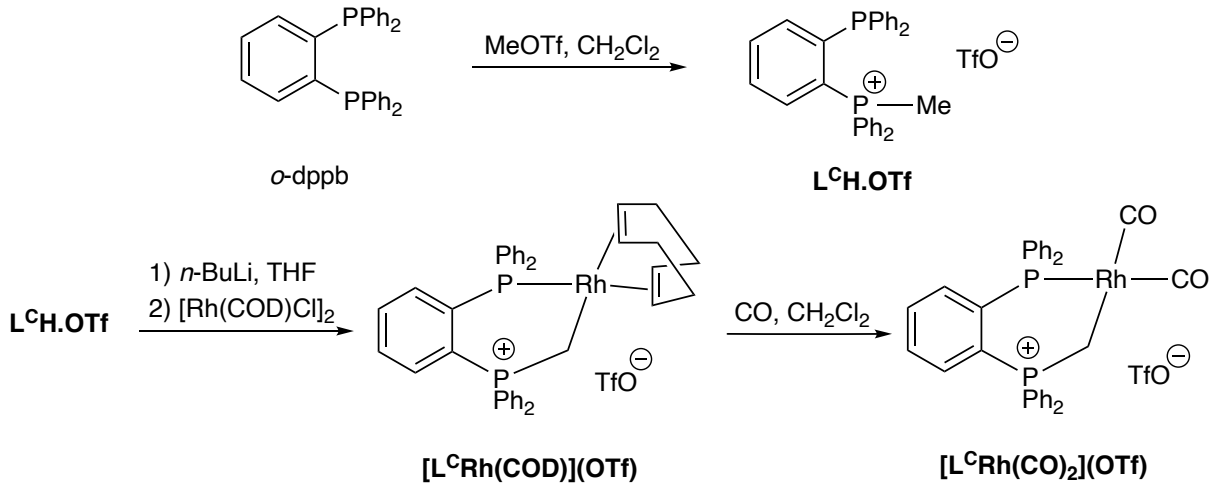

Scheme 1. Synthesis of complex **[L^{C}Rh(CO)$_2$](OTf)** exhibiting a *cis*-chelating phosphine-phosphonium ylide ligand from *o*-diphenylphosphinobenzene (*o*-dppb).

The structure of **[L^{C}Rh(CO)$_2$](OTf)** was unambiguously confirmed by X-ray diffraction (XRD) analysis of yellow crystals deposited from CH_2Cl_2/pentane at –20°C (Figure 3, *right*).[19] As expected, the XRD analysis confirms that the phosphine-phosphonium ylide ligand acts a *cis*-chelating agent and the Rh^{I} atom is located in a quasi square-planar environment. More specifically, the coordination plane is defined by the ylidic C1, the phosphine P2, and the carbonyl C8-C9 donor atoms. The six-membered metallacycle adopts an envelope type-conformation with the rhodium and the ylidic atoms being on the same side of the mean plane defined by the two P-atoms and the phenylene ring. The P−Rh (P2−Rh1 = 2.3235(6) Å) and C_{ylide}−Rh (C1−Rh1 = 2.131(2) Å) bond distances fall within the range of those reported in related Rh(I) complexes.[20] The shortening of the Rh−CO bond (1.886(3) Å) along with the lengthening of the C−O bond (1.136(3) Å) *trans* to the ylide with respect to the Rh−CO (1.921(3) Å) and C−O bonds (1.128(3) Å) *trans* to the phosphine are consistent with the stronger σ-donating vs π-accepting character of the former donor.

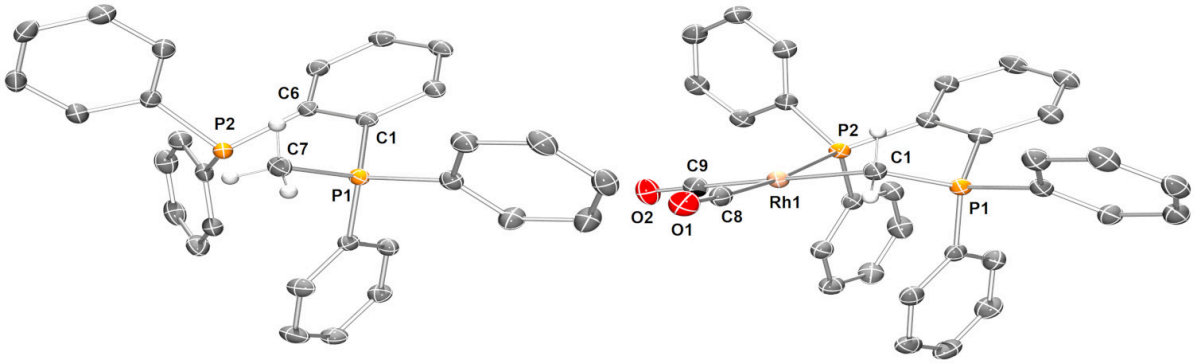

Figure 3. ORTEP plots of **L^{C}.H^{+}** (*left*) and of **[L^{C}Rh(CO)$_2$]$^{+}$** (*right*) (with thermal ellipsoids drawn at the 30% probability level). The H atoms and TfO anion are omitted for clarity. Selected bond lengths [Å] and angles [°]: **L^{C}H.OTf**: P1−C7 = 1.7962(14); C1−P1−C7 = 113.82(6); C6−C1−P1 = 120.44(10); **[L^{C}Rh(CO)$_2$](OTf)**: P1−C1 = 1.757(2); C1−Rh1 = 2.131(2); P2−Rh1 = 2.3235(6); Rh1−C8 = 1.921(3); Rh1−C9 = 1.886(3); C8−O1 = 1.128(3); C9−O2 = 1.136(3); P1−C1−Rh1 = 115.77(11); C1−Rh1−C9 = 178.27(9); P2−Rh1−C8 = 173.56(7); C1−Rh1−P2 = 93.79(6); C8−Rh1−C9 = 92.97(10).

Synthesis and Spectroscopic Characterization of *cis*-[Phosphine-Iminophosphorane Rh^{I}] Complexes.

The phosphino-aminophosphonium salt **L^{N}H.BF$_4$** was obtained in a two-step sequence from readily available triphenylphosphine as previously described.[21] In a first step, the isopropylaminophosphonium was formed by a modified Kirsanov reaction. Then, the phosphine group was introduced through a selective *ortho*lithiation followed by trapping with Ph_2PCl. Finally, washing with an acidic aqueous solution allowed to obtain the targeted phosphino-aminophosphonium **L^{N}H.BF$_4$**, thus controlling the nature of the counter-anion. The phosphine-iminophosphorane Rh complexes were prepared using a similar procedure as for their phosphine-phosphonium ylide counterparts. The deprotonation of **L^{N}H.BF$_4$** was conducted in THF at room temperature with one equivalent of KHMDS (Scheme 2). The formation of **L^{N}** was evidenced by *in situ* $^{31}P\{^{1}H\}$ NMR showing 2 doublets at $\delta_P = -1.2$ ppm and $\delta_P = -13.7$ ppm ($J_{PP} = 13.0$ Hz). After removal of the potassium salt and THF, **L^{N}** was reacted with one equivalent of $[Rh(COD)_2](BF_4)$ in CH_2Cl_2 leading to **[L^{N}Rh(COD)](BF$_4$)**, forming an orange solid which has been isolated in 80% yield. Its $^{31}P\{^{1}H\}$ NMR spectrum shows a doublet of doublets at $\delta_P = 26.6$ ppm for P^{III} ($J_{RhP} = 159.0$ Hz and $J_{PP} = 25.0$ Hz) and a doublet at $\delta_P = 22.7$ ppm for P^{V} nuclei.

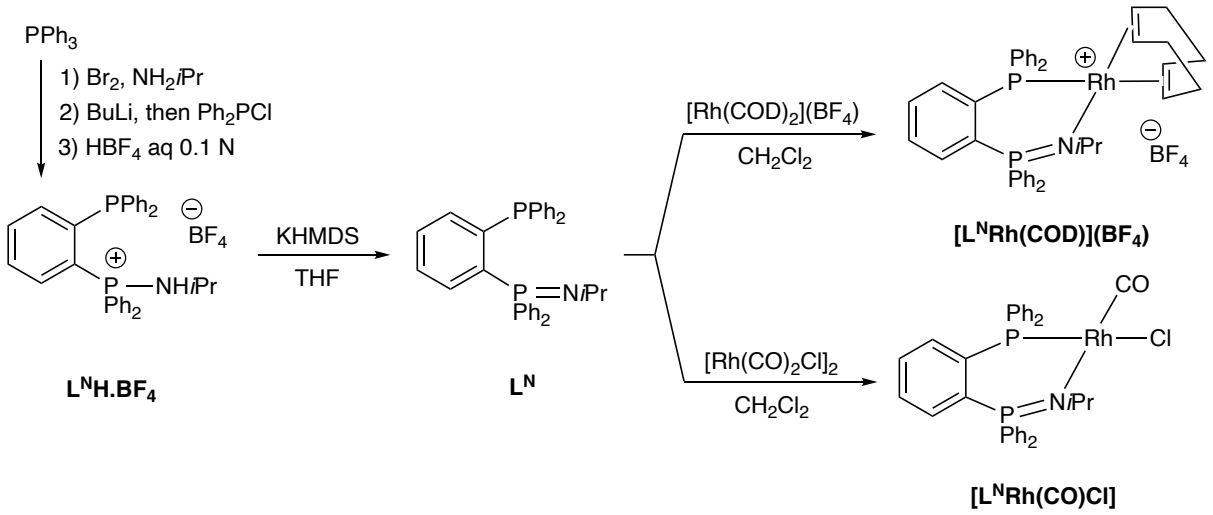

Scheme 2. Synthesis of Rh^{I} complexes **[L^{N}Rh(COD)](BF$_4$)** and **[L^{N}Rh(CO)Cl]** from PPh_3.

The structure of **[L^{N}Rh(COD)](BF$_4$)** was unambiguously confirmed by XRD analysis of the single crystals obtained from CH_2Cl_2/pentane at room temperature. The resolution evidenced 2 disordered structures differing by the position of the Rh and N atoms as well as *i*Pr and COD groups. The ortep plots are shown in Figure 4 (Molecule A, 84.65%) and Figure S1 (Molecule

B, 15.35%), while only the parameters for the major conformer (A) are commented. The Rh atom is tetracoordinated with, as expected, a *cis* arrangement of the phosphine-iminophosphorane ligand and the two olefinic bonds of the COD ligand. It exhibits a distorted square planar geometry (torsion angle N1−P2−$M_{8\text{-}9}$−$M_{12\text{-}13}$: 20.38°, with $M_{8\text{-}9}$ and $M_{12\text{-}13}$ being the centroids of C8−C9 and C12−C13, respectively). The distance between these centroids and the metal center was measured at 2.018 and 2.157 Å, which is comparable with the distance reported by Elsevier and coworkers in a bis(iminophosphorane)methane Rh(COD)$^+$ complex.[22] In **[L^{N}Rh(COD)](BF$_4$)**, the Rh−N1 and Rh−P2 bonds were measured at 2.139(6) and 2.2801(14) Å, respectively. While the Rh−N1 bond distance is comparable to those measured by Elsevier,[22] the P−N bond is in our case slightly longer (1.635(6) Å) than for the bis(iminophosphorane) complex (1.601 Å on average). This different geometrical arrangement suggests slightly weaker interaction between P and N atoms in our system.

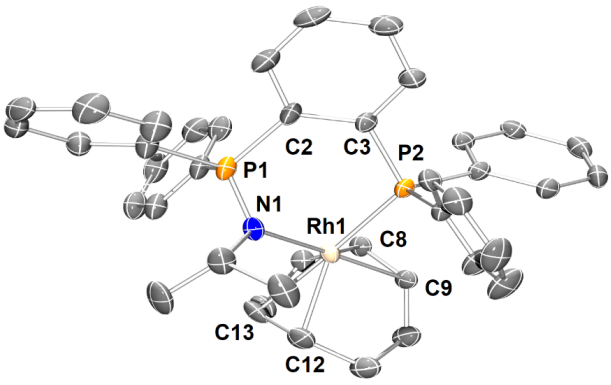

Figure 4. ORTEP plot of **[L^{N}Rh(COD)]**$^+$ (Molecule A). Thermal ellipsoids are drawn at the 50% probability level. The H atoms and BF_4 anion are omitted for clarity. Selected bond lengths (Å) and angles (°): Rh1−N1 2.139(6), Rh1−P2 2.2801(14), Rh1−C8 2.111(6), Rh1−C9 2.157(6), Rh1−C12 2.236(7), Rh1−C13 2.288(6), P1−N1 1.635(6), P1−C2 1.810(6), C2−C3 1.417(7), C3−P2 1.818(5), C8−C9 1.385(9), C12−C13 1.362(10), N1−Rh−P2 87.72(15), N1−Rh1−C12 98.2(2), N1−Rh1−C13 93.5(2), C8−Rh1−P2 95.67(19), C9−Rh1−P2 91.72(19).

The dicarbonyl rhodium complex was obtained by bubbling CO in a CH_2Cl_2 solution of **[L^{N}Rh(COD)](BF$_4$)** in 85% yield (Scheme 3, path a). The ligand substitution induces a shielding of the phosphine NMR signal appearing as a doublet of doublets at δ_P = 13.7 ppm while the iminophosphorane is slightly deshielded resonating at δ_P = 28.7 ppm as a doublet (J_{PP} = 28.5 Hz). Therefore, as with the **L^C** ligand an inversion of the relative position of the ^{31}P NMR resonances compared to the Rh(COD) complex is observed, while the PP coupling

constant remains constant and the J_{RhP} decreases (129.0 Hz). The $^{13}C\{^{1}H, ^{31}P\}$ NMR spectrum evidenced 2 CO resonances at δ_C = 183.9 and 181.7 ppm with a J_{RhC} constant of 64.5 and 61.5 Hz, respectively.

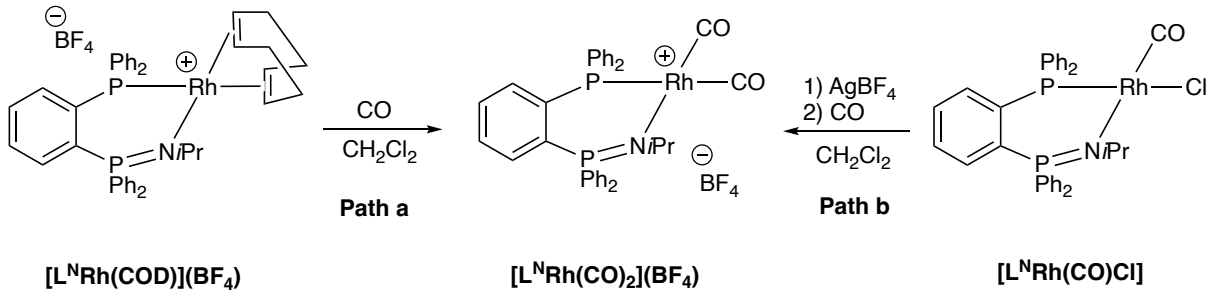

Scheme 3. Preparation of **[L^NRh(CO)$_2$](BF$_4$)** complex following two different pathways.

This is in good agreement with the data reported by Hayes' group for a rhodium dicarbonyl complex supported by a κ^2-bis(iminophosphorane)pyrrole ligand.[23] The IR spectrum of **[L^NRh(CO)$_2$](BF$_4$)** in CH_2Cl_2 shows 2 bands at 2084 and 2018 cm^{-1}, which agrees well with those reported by Hayes and coworkers, as well as a weaker signal at 1987 cm^{-1}. We reasoned that the presence of the additional band may be the result of a dynamic process involving the loss of one carbonyl ligand. Indeed, Hayes and coworkers have isolated both mono- and dicarbonyl rhodium complexes[23] depending on the coordination mode of the bis(iminophosphorane) ligand (κ^3 vs κ^2 respectively). In our case, the hypothetical **[L^NRh(CO)$^+$]** complex should be present in small amount since no other coordinating functions nor solvent molecules could, *a priori,* complete the coordination sphere of the metal.[24] We tried to confirm this assumption by variable temperature $^{31}P\{^{1}H\}$ NMR spectroscopy but the spectra were not temperature dependent (Figure S27). The difference in the results obtained by NMR and IR techniques can be tentatively explained here by the different spectroscopic resolution and the nature of the active group. Indeed, it is much easier and faster to observe the CO vibration rather than the resonance of its quaternary carbon. However, the XRD analysis of **[L^NRh(CO)$_2$](BF$_4$)** also supports the hypothesis of the lability of one of the carbonyl fragments. Indeed, most of the single crystals grown from THF or CH_2Cl_2 solution did not allow to converge to a satisfactory resolution concerning the carbonyl *trans* to the phosphine group (6 attempts on different crystal batches) while the metric and angular data obtained for the rest of the molecule were comparable and meaningful. Finally, we obtained higher quality data on a last crystal batch thanks to a long collection on a more advanced diffractometer. The resulting crystal structure is shown in Figure 5. The behavior of the CO *trans* to P clearly differ from that

trans to the iminophosphorane (vide infra). In **[L^{N}Rh(CO)$_2$](BF$_4$)**, the Rh atom exhibits a distorted square-planar geometry with only a weak deviation from planarity. The P2−C1−C8−N1 angle measures 3.06°. The P−N bond distance is shorter (1.598(3) Å) while the Rh−P2 bond is slightly elongated (2.3086(11) Å) than in **[L^{N}Rh(COD)](BF$_4$)** (1.635(6) and 2.2801(14) Å, respectively). The coordination angle N1−Rh1−P2 is much wider (93.95(9)°) than in **[L^{N}Rh(COD)](BF$_4$)** (87.72(15)°). More generally, it is difficult to compare this structure with literature precedents as examples of iminophosphorane-based Rh(CO)$_2$ complexes are quite rare in the CCDC (8 examples),[25] all being supported by LX and not L$_2$-type ligands. The carbonyl ligands as stated before are markedly different. The Rh−C and C−O bond lengths for the CO *trans* to the phosphine are respectively among the longest (Rh1−C8 1.943(5) Å) and shortest (C8−O8 1.073(5) Å) ones found in the CCDC for Rh(CO)$_2$ complexes.[26] They are also respectively longer (Rh−CO) and shorter (C−O) than those measured in **[L^{C}Rh(CO)$_2$](OTf)** (1.921(3) and 1.128(3) Å). The long Rh−CO distance is in agreement with its proposed lability which is also supported by molecular modeling data. The carbonyl *trans* to the iminophosphorane exhibits parameter close to those measured in **[L^{C}Rh(CO)$_2$]$^+$** with a comparable C−O bond length 1.134(4) Å vs 1.136(3) Å. Conversely, the Rh−C1 bond (1.840(4) Å) is shorter than in the phosphonium ylide complex (1.886(3) Å) and appears in the lower range of the previously reported structures (1.838−1.922 Å). This may indicate a strong donation from Rh to CO in agreement with the quasi-linear arrangement of these atoms (Rh1−C1−O1: 176.3(4)°).

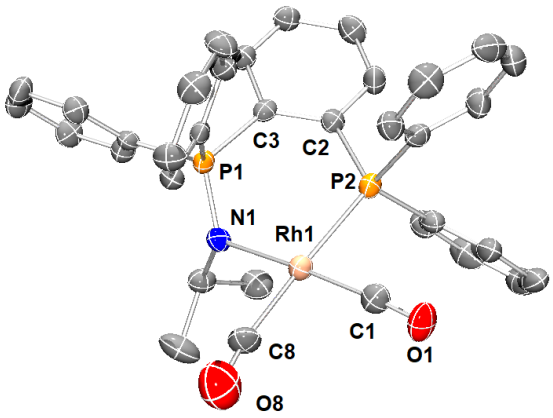

Figure 5. ORTEP plot of **[L^{N}Rh(CO)$_2$](BF$_4$)**.Thermal ellipsoids are drawn at the 50% probability level. H atoms are omitted for clarity. Selected bond lengths (Å) and angles (°): Rh1−N1 2.118(3), Rh1−P2 2.3086(11), Rh1−C1 1.840(4), C1−O1 1.134(4), Rh1−C8 1.943(5), C8−O8 1.073(5), P1−N1 1.598(3), P1−C3 1.821(4), C2−C3 1.409(5), C2−P2 1.832(4), C1−Rh1−P2 87.77(13), N1−Rh1−P2 93.95(9), C1−Rh1−N1 176.74(16), C8−Rh1−P2 175.99(13), O1−C1−Rh1 176.3(4), O8−C8−Rh1 171.1(4).

As an additional proof concerning the secondary CO band observed in the IR spectrum, we prepared **[L^{N}Rh(CO)$_2$](BF$_4$)** following a different protocol via a ligand substitution from the **[L^{N}Rh(CO)Cl]** complex (Scheme 3, path b). The synthesis of **[L^{N}Rh(CO)Cl]** was performed by the addition of half an equivalent of $[Rh(CO)_2Cl]_2$ to a CH_2Cl_2 solution of **L^N** (Scheme 2). The title complex was isolated in 49% yield because of loss during the workup. This neutral complex exhibits two ^{31}P resonances a doublet at δ_P = 19.7 and a doublet of doublets at δ_P = 36.1 ppm (J_{RhP} = 180.5 Hz and J_{PP} = 26.5 Hz) for the P^{III} and P^V nuclei, respectively. Those data are in perfect agreement with those reported by Cavell and coworkers for a similar complex featuring an aryl substituent on the N atom.[27] The deshielding of the P^V nucleus as well as the J_{RhP} constant in **[L^{N}Rh(CO)Cl]** are larger than in the cationic dicarbonyl complex. The CO ^{13}C signal was observed at δ_C = 188.1 ppm in the $^{13}C\{^1H, ^{31}P\}$ NMR spectrum recorded in CD_2Cl_2. Unfortunately, Cavell and coworkers did not observe the CO NMR resonance for the comparable complexes they prepared.[27,28] The IR CO stretching frequency of **[L^{N}Rh(CO)Cl]** in CH_2Cl_2 was measured at 1972 cm^{-1} slighlty lower than the value reported by Cavell's group for the P=NTMS complex.[28] This may indicate a stronger electron transfer from the metal to the CO in agreement with the X-ray data (vide infra).

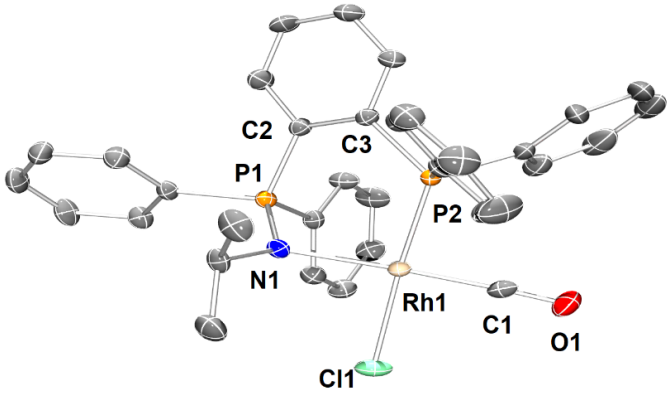

Figure 6. ORTEP plot of **[L^{N}Rh(CO)Cl]**. Thermal ellipsoids are drawn at the 50% probability level. H atoms are omitted for clarity. Selected bond lengths (Å) and angles (°): Rh1−N1 2.120(3), Rh1−P2 2.2108(8), Rh1−Cl1 2.3929(9), Rh1−C1 1.817(4), C1−O1 1.137(5), P1−N1 1.589(3), P1−C2 1.824(3), C2−C3 1.403(5), C3−P2 1.841(3), C1−Rh−Cl1 87.04(11), C1−Rh1−P2 89.52(11), N1−Rh1−P2 92.34(8), N1−Rh1−Cl1 91.00(8).

The XRD structure of **[L^{N}Rh(CO)Cl]** confirms a square-planar geometry with only a very limited deviation to planarity of 0.71° (Figure 6). The chloride ligand is localized *trans* to the phosphine as was observed by Cavell's group for a comparable Rh(CO)Cl complex featuring a

trimethylsilyl group on the nitrogen.[28] The Rh−P, Rh−Cl, and P−N bond lengths are also comparable with those previously reported. However, we observed shorter Rh−N and Rh−C bonds (2.120(3) and 1.817(4) Å), together with a longer C−O bond (1.137(5) Å). This can probably be explained by the difference in the electronic properties of the iminophosphorane. Indeed, Cavell and coworkers employed a TMS substituent leading to an iminophosphorane which is less electron-rich than the one we used. Thus, in our case, the electron transfer from N to the metal and then from Rh to the carbonyl ligand is stronger. The angles around the Rh are close to 90°, comparable with the previously published data.

From **[L^{N}Rh(CO)Cl]** we then generated *in situ* **[L^{N}Rh(CO)](BF$_4$)** by addition of one equivalent of $AgBF_4$, the clean formation of this complex was ascertained by *in situ* $^{31}P\{^1H\}$ NMR spectroscopy showing a doublet of doublets at δ_P = 49.1 ppm for the P^{III} nucleus (J_{RhP} = 214.5 Hz, J_{PP} = 17.5 Hz) and a doublet at δ_P = 26.9 ppm for the PN moiety (Scheme 3, path b, Figure S28). The large increase in the J_{RhP} constant (214.5 vs 129.0 Hz) in **[L^{N}Rh(CO)](BF$_4$)** may result from a stronger P−Rh binding due to the electron deficiency of the Rh center. The IR spectrum recorded from a CH_2Cl_2 solution evidences a strong band at 1980 cm^{-1} close to the additional band we observed in the IR spectrum of **[L^{N}Rh(CO)$_2$](BF$_4$)** (ca. 1987 cm^{-1}). Finally, we saturated the CH_2Cl_2 solution of the *in situ* generated **[L^{N}Rh(CO)](BF$_4$)** with CO and we observed the formation of **[L^{N}Rh(CO)$_2$](BF$_4$)** both by $^{31}P\{^1H\}$ NMR and *in situ* IR spectroscopy. In this latter experiment the IR band at 1987 cm^{-1} only appears as a shoulder probably because of the excess CO present in the solution which must influence the reaction outcome favoring the $Rh(CO)_2$ species, hence reinforcing our interpretation.

IR Spectroscopy, Cyclic Voltammetry, and DFT Studies of *cis*-[Phosphine-Ylide Rh^I] Complexes.

As P-ylides behave as strong electron donating ligands, a significant back donation from metal to carbonyl is expected. It results in short Rh−C and long C−O bonds. Data obtained for **[L^{C}Rh(CO)$_2$]$^+$** and **[L^{N}Rh(CO)$_2$]$^+$** (Table 1, lines 1-2) show shorter Rh−C in the iminophosphorane $Rh(CO)_2$ complex compared to the related phosphonium ylide $Rh(CO)_2$ complex but the C−O bonds are comparable. This might be explained by a certain lability of one CO co-ligand and/or by the effect of the σ-donating N-*i*Pr substituent in the iminophosphorane representative. Molecular modeling was thus conducted on these ylidic systems in order to answer those questions. As shown in Table 1 (lines 3-4), the agreement between the optimized structural parameters of **[L^{C}Rh(CO)$_2$]$^+$** and **[L^{N}Rh(CO)$_2$]$^+$** and those obtained from XRD is satisfying. Most notably, the trend of the Rh−C and C−O bond lengths in passing from P^+-C^- to P=N systems is reproduced.

Table 1. Selected Experimental and Calculated Structural Data, and HOMO-LUMO gap for Carbonylrhodium Complexes.[a]

Complexes	Rh−CO[b]	C−O[b]	Rh−C−O[b]	P−N/C	N/C−Rh	P−Rh	HOMO-LUMO gap
$^{Exp.}$**[L^{C}Rh(CO)$_2$]$^+$**	1.886(3)	1.136(3)	178.27(9)	1.757(2)	2.131(2)	2.3235(6)	-
$^{Exp.}$**[L^{N}Rh(CO)$_2$]$^+$**	1.840(4)	1.134(4)	176.3(4)	1.598(3)	2.118(3)	2.3086(11)	-
$^{Calcd.}$**[L^{C}Rh(CO)$_2$]$^+$**	1.915	1.176	177.4	1.844	2.143	2.441	4.11
$^{Calcd.}$**[L^{N}Rh(CO)$_2$]$^+$**	1.884	1.177	179.1	1.706	2.105	2.474	3.55
$^{Calcd.}$**[L^{Cipr}Rh(CO)$_2$]$^+$**	1.908	1.176	176.0	1.875	2.172	2.451	4.12
$^{Calcd.}$**[L^{Cipr2}Rh(CO)$_2$]$^+$**	1.908	1.178	171.2	1.946	2.228	2.476	4.21
$^{Calcd.}$**[L^{NH}Rh(CO)$_2$]$^+$**	1.894	1.176	177.7	1.706	2.105	2.474	3.92

[a] Geometry optimization was performed at DFT level using B3LYP functional and LANLDZ basis set as specified in the Computational Details. Bond lengths are in Å, angles in degrees, and HOMO-LUMO gap in eV. [b] CO *trans* to the ylidic coordinating atom.

We have also calculated using B3LYP functional and LANL2DZ basis the optimized structures of Rh complexes with one **[L^{Cipr}Rh(CO)$_2$]$^+$** and two **[L^{Cipr2}Rh(CO)$_2$]$^+$** isopropyl substituents at the ylidic carbon atom as well as the P=NH parent complex **[L^{NH}Rh(CO)$_2$]$^+$** (Table 1, lines 5-7). Unexpectedly, these calculations show that the change of the substituent of the coordinating ylidic atom has only marginal influence on the Rh−C and C−O bond lengths even if the global tendency goes in the right direction. Of note, the introduction of two bulky i*P*r substituents on the C-ylidic center also causes a significant perturbation of the Rh−C−O angle value (Table 1, line 6).

The corresponding frontiers Khon-Sham orbitals are reported in SI (Figure S2). For **[L^{N}Rh(CO)$_2$]$^+$**, the HOMO orbital develops on the Rh d-shell and the iminophosphorane fragment, while in the case of **[L^{C}Rh(CO)$_2$]$^+$** the HOMO is a pure metal d orbital. In both ylidic systems, the LUMO orbitals are concentrated on the coordination sphere (π*CO) with a

participation of the metal. The HOMO/LUMO gap is calculated at 3.55 and 4.11 eV for $\mathbf{[L^{N}Rh(CO)_2]^+}$ and $\mathbf{[L^{C}Rh(CO)_2]^+}$, respectively (Table 1). The larger HOMO/LUMO gap in C-ylidic systems is due to the lower HOMO and to a lesser extent to the slightly higher LUMO.

The calculated antisymmetric and symmetric CO stretching peaks for the two synthesized complexes were found at 1924 and 1994 cm^{-1} for $\mathbf{[L^{C}Rh(CO)_2]^+}$ and at 1930 and 2003 cm^{-1} for $\mathbf{[L^{N}Rh(CO)_2]^+}$, respectively (Table 2). Note that the former represent purely harmonic frequencies, and no empirical scaling factor has been applied, hence they are obviously shifted compared to the experimental values. Nevertheless, calculations as experiments point out the close similarities of the CO vibrations in the two different environments. However, the relative magnitude of the measured average CO frequency (2051 vs 2053 cm^{-1} for $\mathbf{L^{N}}$ and $\mathbf{L^{C}}$ complexes, respectively) does not match with the calculated values giving a higher average CO frequency for the $\mathbf{L^{N}}$ complex (1966 vs 1959 cm^{-1}). This may be explained by the weak coordination of one CO in $\mathbf{[L^{N}Rh(CO)_2]^+}$ that could influence the bonding between the metal and the remaining CO. Furthermore, a satellite peak on the doublet region which is absent from the spectrum of $\mathbf{[L^{C}Rh(CO)_2]^+}$ and is not recovered in the DFT modeling is observed in the $\mathbf{[L^{N}Rh(CO)_2]^+}$spectrum. While the satellite band could be ascribed to anharmonic or overtones effects, as already discussed, the presence of parasite Rh(CO) species is a more sounding hypothesis. Thus, we performed molecular modeling on a complex in which one CO ligand is removed or substituted either by a Cl^- or BF_4^- forming an ion couple. We found vibrational frequencies for the remaining coordinated CO of 1886 cm^{-1} (COCl), 1900 (only one CO), and 1906 cm^{-1} (BF_4^- ionic couple) (Table 2). Thus, while the precise nature of that metallic compound could not be resolved due to the close spectral signature, the calculated frequencies fits with that of the satellite peak, which is due to a mono-Rh(CO) adduct and, hence, can be disregarded in the following analysis.

Having explained the presence of the satellite peak, the close similarity of the vibrational frequencies of the two complexes should still be rationalized. Importantly, there is a further difference in the two chemical structures compared henceforth, namely the nature of the substituent appended to either the nitrogen or the carbon complexing the Rh atom. Indeed, while a rather strong donor group, i.e. isopropyl, is appended to $\mathbf{[L^{N}Rh(CO)_2]^+}$ only hydrogen atoms are present in $\mathbf{[L^{C}Rh(CO)_2]^+}$. In this respect, to disentangle the effects of the substituent we have also calculated the CO stretching vibrations for the iminophosphorane complex featuring only a NH unit $\mathbf{[L^{NH}Rh(CO)_2]^+}$, and those of the ylide complexes with one $\mathbf{[L^{Cipr}Rh(CO)_2]^+}$ and two $\mathbf{[L^{Cipr2}Rh(CO)_2]^+}$ isopropyl chains on carbon. In the P=N case, the difference observed with the parent compound remains negligible. However, the CO vibrational frequencies are blue shifted by 4 and 3 cm^{-1} for the antisymmetric and symmetric stretching, respectively (Table

2) when suppressing the alkyl substituent. In the P^{+}–C^{-} case, the antisymmetric vibration is red-shifted by 3 and 17 cm^{-1} after the inclusion of one or two i*P*r substituents while the symmetric stretching frequency follows the same trend being diminished by 5 and 16 cm^{-1}, respectively. From these data it is evident that the peripheral ligand is non-innocent and may significantly alter the electron density organization of the parent compound. More specifically, the presence of one isopropyl in **$[L^{N}Rh(CO)_2]^{+}$** seems sufficient to almost compete with the strong donating ability of **$[L^{C}Rh(CO)_2]^{+}$** ultimately providing similar spectroscopic signatures.

The behavior of **$[L^{C}Rh(CO)_2]^{+}$** and **$[L^{N}Rh(CO)_2]^{+}$** complexes was then investigated by cyclic voltammetry. Two oxidations and one reduction, all irreversible, were observed in both series. The reduction of **$[L^{N}Rh(CO)_2](OTf)$** (E_P^{red1} = –1.35 V vs SCE) was found to be easier than that of **$[L^{C}Rh(CO)_2](BF_4)$** (E_P^{red1} = –1.56 V vs SCE) in agreement with the higher energy of the LUMO (vide supra, Figure S2) of the phosphonium-ylide complex. Moreover, the first oxidation of the P=N complex occurs at a sligthly less anodic potential (E_P^{ox1} = 1.17 V vs SCE) than that of the P^{+}–C^{-} complex (E_P^{ox1} = 1.29 V vs SCE), while the second irreversible oxidation takes place at the same potential (1.66 V vs SCE) for both complexes. The first oxidation potentials fits well with the energy order determined for the HOMOs.

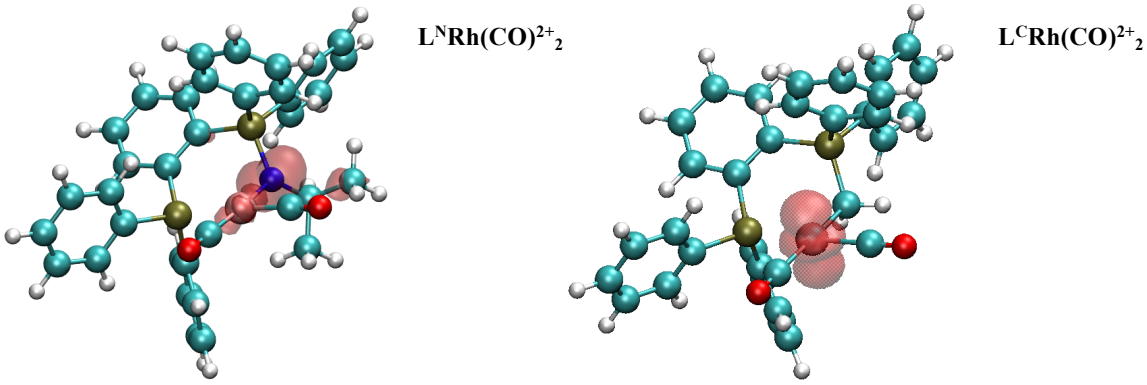

Figure 7. DFT spin density obtained for the oxidized **$[L^{N}Rh(CO)_2]^{+}$** and **$[L^{C}Rh(CO)_2]^{+}$** complexes at the respective equilibrium geometries.

The profile of the first oxidation wave is well reproduced by molecular modeling which yielded a higher potential for **$[L^{C}Rh(CO)_2]^{+}$** than for **$[L^{N}Rh(CO)_2]^{+}$**, the difference between the two potentials being about 0.16 V compared to the 0.12 V observed experimentally (Table 2). Interestingly as shown in Figure 7, the oxidation is centered on two different chemical moieties for the two Rh complexes. Indeed, in agreement with the nature of the HOMOs (Figure S2), while the spin density, i.e. the density of the unpaired electron in the oxidized species, is

centered on the metal d-orbital for $[L^{C}Rh(CO)_2]^{2+}$, in the case of $[L^{N}Rh(CO)_2]^{2+}$ the oxidation takes place on the N coordinating atom with only a minor participation of the metal.

Table 2. Experimental and Calculated IR CO Stretching Frequencies (cm^{-1}), and E_P^{ox} for Carbonylrhodium Complexes.[a]

Complexes	ν_{CO} (exp)	av. (exp)	ν_{CO} (calcd)	av. (calcd)	Δav. (exp-calcd)	E_P^{ox1}[b] (exp)	E^{ox1}[b] (calcd)
$[L^{C}Rh(CO)_2]^{+}$	2024, 2082	2053	1924, 1994	1959	94	1.29	1.63
$[L^{N}Rh(CO)_2]^{+}$	2018, 2084 1987	2051	1930, 2003	1966	85	1.17	1.47
$[L^{Cipr}Rh(CO)_2]^{+}$	-	-	1921, 1989	1955	-	-	
$[L^{Cipr2}Rh(CO)_2]^{+}$	-	-	1907, 1978	1942	-	-	
$[L^{NH}Rh(CO)_2]^{+}$	-	-	1934, 2006	1970	-	-	
$[L^{N}Rh(CO)Cl]$	1972	-	1886	-	86	-	

[a] Geometry optimization was performed at DFT level using B3LYP functional and LANL2DZ basis as further specified in the Computational Details. [b] Both experimental and calculated Ep^{ox1} values (V) are given vs SCE.

To better understand the electronic structures, and the effects of the peripheral ligand, we also report in Table 3 the Natural Population Analyses (NPA) atomic charges calculated for each ylidic $Rh(CO)_2$ complex. Again, we may see how both the positive character of the P atoms and the negative density on C or N atoms are strongly dependent on the nature of the peripheral ligand, and more precisely on the ylidic substituent. Interestingly, this variation appears non-local and is also transferred to the Rh as well as to the CO co-ligands, hence justifying the evolution of their spectroscopic properties. However, some discrepancies in the trend of the charges can be outlined. This should be ascribed to different issues, and namely to the fact that atomic point charges are not physical observable, and consequently their value strongly depends on the chosen partition strategy. Furthermore, the inclusion of two isopropyl groups induces a rather crowded coordination sphere which leads to some structural

deformations to partially release the sterical tension. These variations in the equilibrium geometry also have a non-negligible effect on the calculated charges. However, when comparing unsubstituted systems (i.e. $P^{+}–CH_2^{-}$ *vs* P=NH) where the steric effect of the ylidic substituent can be neglected, the charge values indicate that the phosphonium ylide transfers more electron density to the Rh center and ultimately to the CO moieties, the CO *trans* to the ylide being naturally more impacted. As expected, the charge of the P-atom of the phosphine donor remains of same order in the two families of ylide. As shown in SI (Table S8) the effect of the basis set is modest in the distribution of the charges and thus the tendency we have evidenced cannot be considered a simple computational artifact.

Table 3. Principal NPA charges of dicarbonyl rhodium Complexes.

Complexes	$[L^{C}Rh(CO)_2]^{+}$	$[L^{Cipr}Rh(CO)_2]^{+}$	$[L^{Cipr2}Rh(CO)_2]^{+}$	$[L^{N}Rh(CO)_2]^{+}$	$[L^{NH}Rh(CO)_2]^{+}$
Rh	-0.561	-0.552	-0.482	-0.411	-0.391
N/C	-0.978	-0.741	-0.477	-1.053	-1.254
P(Rh)[a]	1.063	1.073	1.027	1.062	1.060
P(N/C)[a]	1.504	1.490	1.445	1.737	1.737
CO_1[b]	0.260	0.241	0.206	0.253	0.271
CO_2[b]	0.218	0.220	0.213	0.131	0.234

[a] P(Rh) and P(N/C) identify the P-atom bound to the metal and the iminophosphorane/ylide, respectively. [b] CO_1 represent the CO *trans* to the coordinating P-atom and CO_2 the CO *trans* to the iminophosphorane/ylide atom.

CONCLUSION

With the aim to compare the donating ability of iminophosphorane and phosphonium ylide ligands, we synthesized and investigated new cationic Rh^{I} dicarbonyl complexes featuring a mixed *cis*-chelating phosphine-donor ligand built on a rigid *ortho*-phenylene skeleton and differing by the nature of the donor group, the latter being either a phosphonium ylide ($P^{+}–CH_2^{-}$) or an iminophosphorane (P=N*i*Pr). We observe significant differences in the chemical behavior of these two complexes, and notably, the iminophosphorane representative presented a certain lability for one of the CO groups. This fact may indicate that accommodating two carbonyl groups for the cationic Rh center stabilized by the iminophosphorane ligand is more difficult than for the neutral Rh coordinated to the ylide ligand. Indeed, in the latter case the positive charge of the complex is localized on the phosphonium fragment, i.e. distant from the

metallic center. Nevertheless the spectrocopic data for both experimentally prepared complexes are rather similar suggesting comparable electron-donating ability. In order to further understand this result, we resort to molecular modeling at Density Functional Theory (DFT) level. It confirms the similarity of the spectroscopic properties between the two derivatives. Nevertheless, our simulations also underline the influence of the *i*Pr substituent on the N atom of the iminophosphorane. Indeed, the alkyl substituent allows the iminophosphorane to compete in terms of donating ability with the $P^+–CH_2^-$ ylide-based moiety. If the role of the accessory ligands is often overlooked our results evidence novel possibilities to specifically tune the properties of organometallic compounds, adding more flexibility to their design. Indeed, while achieving P=NH or substituted $P^+–CHR^-$ is synthetically more challenging than obtaining substituted iminophosphorane and unsubstituted phosphonium ylides, this study suggests that these two types of strongly electron-donating phosphorus-based ligand can be highly complementary. They may be valuable assets in the toolbox of coordination chemists since they present close electronic properties with a different steric pattern. The original properties of this type of organometallic complexes may in particular be highly beneficial for further applications especially in the field of catalysis. A direction to which we plan to focus our future work exploiting the potentiality of our original organometallic systems.

EXPERIMENTAL SECTION

General Remarks. All manipulations were performed under an inert atmosphere of dry nitrogen by using standard vacuum line and Schlenk tube techniques. Glassware was dried at 120 °C in an oven for at least three hours. Dry and oxygen-free organic solvents (THF, Et_2O, CH_2Cl_2, toluene, pentane) were obtained using a LabSolv (Innovative Technology) or (MBraun-SPS) solvent purification system. Acetonitrile was dried and distilled over P_2O_5 under argon. Phosphine-aminophosphonium $\mathbf{L^NH.BF_4}$ was synthesized as previously described.[21] All other reagent-grade chemicals were purchased from commercial sources and used as received. Chromatographic purification was carried out on silica gel (SiO_2, 63−200 μm). ^1H, ^{31}P, and ^{13}C NMR spectra were obtained on Bruker AC300 SY, AV300, AV400 or NEO600 spectrometers. NMR chemical shifts δ are indicated in ppm, with positive values to high frequency relative to the tetramethylsilane reference for ^1H and ^{13}C and to 85% H_3PO_4 for ^{31}P. If necessary, additional information on the carbon signal attribution was obtained using $^{13}C\{^1H, ^{31}P\}$, *J*-modulated spin−echo (JMOD) $^{13}C\{^1H\}$, $^1H–^{13}C$ HSQC, HMQC, and/or HMBC experiments. Solution IR spectra were recorded in 0.1 mm CaF_2 cells using a Perkin Elmer Frontier FT-IR spectrometer or with an IR-TF Thermo Scientific Nicolet iS5 spectrometer, and are given in cm^{-1}. MS spectra (ESI mode) were performed by the mass spectrometry service of the “Institut

de Chimie de Toulouse" using a Xevo G2 QTof (Waters) spectrometer or recorded in "LCM" with a time-TOF mass spectrometer (Bruker, France) by Dr. S. Bourcier. Elemental analyses were carried out by the elemental analysis service of the "LCC" using a Perkin Elmer 2400 series II analyzer. Voltammetric measurements were performed by the electrochemistry service of the "LCC" with a potentiostat Autolab PGSTAT100 controlled by GPES 4.09 software. Experiments were carried out at room temperature in a homemade airtight three-electrode cell consisting of a Pt working electrode (d = 0.5 mm), a platinum wire (S = 1 cm^2) as counter electrode, and a saturated calomel electrode (*SCE*) separated from the solution by a bridge compartment as a reference. Before each measurement, the working electrode was cleaned with a polishing machine (Presi P230, P4000). The measurements were carried out in dry CH_2Cl_2 under argon atmosphere using 0.1 M [*n*Bu_4N](OTf) or [*n*Bu_4N](BF_4) (Fluka, 99% puriss electrochemical grade) as supporting electrolyte and typically 10^{-3} M sample concentration.

Synthesis of L^CH.OTf pre-ligand.

MeOTf (127 µL, 1.12 mmol) was added at –78 °C to a solution of 1,2-bis(diphenylphosphino)benzene (0.50 g, 1.12 mmol) in CH_2Cl_2 (20 mL). The mixture was then slowly warmed to RT and stirred for 16 hours. After evaporation of the solvent under vacuum and washing with Et_2O (20 mL), the phosphonium **L^CH.OTf** was obtained as a white powder (0.67 g, 98%). Recrystallization from CH_2Cl_2/pentane at RT gave colorless crystals, some of them being suitable for X-ray diffraction study. $^{31}P\{^1H\}$ NMR (162 MHz, CD_3CN, 25 °C): δ = 22.3 (d, J_{PP} = 25.9 Hz, P^+), –15.4 (d, J_{PP} = 25.9 Hz, P); ^1H NMR (400 MHz, CD_3CN, 25 °C): δ = 7.81 (brt, J_{HH} = 8.0 Hz, 1H, CH_{Ar}), 7.73 (brt, J_{HH} = 8.0 Hz, 2H, CH_{Ar}), 7.69–7.54 (m, 10H, CH_{Ar}), 7.45–7.36 (m, 3H, CH_{Ar}), 7.30 (brt, J_{HH} = 8.0 Hz, 4H, CH_{Ar}), 6.99 (brt, J_{HH} = J_{PH} = 8.0 Hz, 4H, CH_{Ar}), 3.10 (dd, J_{PH} = 4.0 and 14.0 Hz, 3H, CH_3); ^{13}C NMR (101 MHz, CD_3CN, 25 °C): δ = 143.7 (dd, J_{PC} = 11.1 and 18.1 Hz, C_{Ar}), 140.0 (d, J_{PC} = 11.1 Hz, CH_{Ar}), 137.6 (dd, J_{PC} = 10.1 and 13.1 Hz, CH_{Ar}), 136.1 (d, J_{PC} = 3.0 Hz, CH_{Ar}), 135.6 (d, J_{PC} = 3.0 Hz, CH_{Ar}), 134.9 (d, J_{PC} = 7.0 Hz, C_{Ar}), 134.1 (d, J_{PC} = 11.1 Hz, CH_{Ar}), 134.0 (d, J_{PC} = 18.1 Hz, CH_{Ar}), 132.0 (d, J_{PC} = 13.1 Hz, CH_{Ar}), 131.0 (d, J_{PC} = 13.1 Hz, CH_{Ar}), 130.5 (s, CH_{Ar}), 129.8 (d, J_{PC} = 7.0 Hz, CH_{Ar}), 127.6 (dd, J_{PC} = 36.2 and 89.5 Hz, C_{Ar}), 122.2 (q, J_{FC} = 319.9 Hz, CF_3), 121.5 (dd, J_{PC} = 2.0 and 89.5 Hz, C_{Ar}), 12.9 (dd, J_{PC} = 19.1 and 59.3 Hz, CH_3); HRMS (ESI^+): 461.1588 calcd for $C_{31}H_{27}P_2^+$ [M - TfO]$^+$, found, 461.1590; Elemental analysis for $C_{32}H_{27}F_3O_3P_2S$: calcd, C 62.95, H 4.46; found, C 62.26, H 4.16.

Synthesis of [L^CRh(COD)](OTf) complex.

*n*BuLi (1.6 M, 108 µL, 0.17 mmol) was added at −78 °C to a solution of phosphonium **L^CH.OTf** (0.10 g, 0.16 mmol) in THF (10 mL). The mixture was then warmed to room temperature and stirred for 15 min. After cooling the solution to −78°C, $[RhCl(COD)]_2$ (40 mg, 0.082 mmol) was added. The mixture was then slowly warmed to RT and stirred for 12 hours. After evaporation of the solvent under vacuum, the crude residue was dissolved in CH_2Cl_2 (15 mL), and the resulting solution was filtered over celite. After evaporation of the solvent under vacuum and washing with Et_2O (10 mL), complex **[L^CRh(COD)](OTf)** was obtained as a yellow powder (120 mg, 90%). Yellow crystals of **[L^CRh(COD)](OTf)** were obtained by recrystallization from CH_2Cl_2/Et_2O at −20 °C. $^{31}P\{^1H\}$ NMR (162 MHz, CD_3CN, 25 °C): δ = 32.7 (dd, J_{PP} = 25.9 Hz and J_{RhP} = 162.0 Hz, P), 28.6 (dd, J_{PP} = 25.9 Hz and J_{RhP} = 4.8 Hz, PCH_2); ^1H NMR (400 MHz, CD_3CN, 25 °C): δ = 7.76 (brt, J_{HH} = 8.0 Hz, 3H, CH_{Ar}), 7.65–7.46 (m, 20H, CH_{Ar}), 7.38–7.31 (m, 1H, CH_{Ar}), 4.87 (brs, 2H, CH_{COD}), 3.51 (brs, 2H, CH_{COD}), 2.13–1.77 (m, 8H, CH_{2COD}), 1.43 (d, J_{PH} = 12.0 Hz, 2H, CH_2); ^{13}C NMR (101 MHz, CD_3CN, 25 °C): δ = 137.3 (d, J_{PC} = 9.0 Hz, CH_{Ar}), 137.1 (d, J_{PC} = 34.2 Hz, C_{Ar}), 136.9 (t, J_{PC} = 10.1 Hz, CH_{Ar}), 134.6 (dd, J_{PC} = 3.0 and 5.0 Hz, CH_{Ar}), 133.9 (d, J_{PC} = 2.0 Hz, CH_{Ar}), 133.7 (d, J_{PC} = 12.1 Hz, CH_{Ar}), 132.8 (d, J_{PC} = 10.1 Hz, CH_{Ar}), 132.1 (dd, J_{PC} = 2.0 and 12.1 Hz, CH_{Ar}), 131.4 (d, J_{PC} = 44.3 Hz, C_{Ar}), 131.3 (d, J_{PC} = 2.0 Hz, CH_{Ar}), 130.0 (d, J_{PC} = 12.1 Hz, CH_{Ar}), 129.4 (dd, J_{PC} = 19.2 and 89.9 Hz, C_{Ar}), 129.3 (d, J_{PC} = 10.1 Hz, CH_{Ar}), 127.1 (d, J_{PC} = 82.5 Hz, C_{Ar}), 121.3 (q, J_{FC} = 320.9 Hz, CF_3), 102.6 (dd, J_{PC} = 11.1 Hz and J_{RhC} = 7.0 Hz, CH_{COD}), 84.9 (d, J_{RhC} = 9.0 Hz, CH_{COD}), 30.9 (d, J_{PC} = 2.0 Hz, CH_{2COD}), 30.0 (s, CH_{2COD}), –2.2 (ddd, J_{PC} = 12.1 and 35.2 Hz, J_{RhC} = 24.1 Hz, CH_2); HRMS (ESI^+): 671.1504 calcd for $C_{39}H_{38}P_2Rh^+$ [M - TfO]$^+$, found, 671.1521; Elemental analysis for $C_{40}H_{38}F_3O_3P_2RhS.(0.4\ CH_2Cl_2)$: calcd, C 56.78, H 4.58; found, C 56.70, H 3.96.

Synthesis of [L^CRh(CO)$_2$](OTf) complex.

Complex **[L^CRh(COD)](OTf)** (0.12 g, 0.147 mmol) was dissolved in CH_2Cl_2 (5 mL), and carbon monoxide was bubbled at room temperature for 15 min. After addition of pentane (15 mL) and elimination of the supernatant, complex **[L^CRh(CO)$_2$](OTf)** was obtained as a yellow powder (0.10 g, 88%). Recrystallization from CH_2Cl_2/pentane at −20 °C gave pale yellow crystals suitable for X-ray diffraction study. $^{31}P\{^1H\}$ NMR (162 MHz, CD_3CN, 25 °C): δ = 27.8 (dd, J_{PP} = 41.3 Hz and J_{RhP} = 4.8 Hz, PCH_2), 21.0 (dd, J_{PP} = 41.3 Hz and J_{RhP} = 129.6 Hz, P); ^1H NMR (400 MHz, CD_3CN, 25 °C): δ = 7.86 (brt, J_{HH} = 8.0 Hz, 1H, CH_{Ar}), 7.73–7.66 (m, 3H, CH_{Ar}), 7.56–7.28 (m, 20H, CH_{Ar}), 1.92 (brd, J_{PH} = 16.0 Hz, 2H, CH_2); ^{13}C NMR (101 MHz, CD_3CN, 25 °C): δ = 186.0 (brs, CO), 184.7 (dd, J_{PC} = 15.6 Hz and J_{RhC} = 58.8 Hz, CO), 137.2

(t, J_{PC} = 8.0 Hz, CH_{Ar}), 137.1 (d, J_{PC} = 7.0 Hz, CH_{Ar}), 135.5 (dd, J_{PC} = 3.0 and 7.0 Hz, CH_{Ar}), 134.5 (d, J_{PC} = 3.0 Hz, CH_{Ar}), 134.0 (d, J_{PC} = 13.1 Hz, CH_{Ar}), 132.9 (dd, J_{PC} = 7.0 and 43.3 Hz, C_{Ar}), 132.7 (d, J_{PC} = 10.1 Hz, CH_{Ar}), 132.3 (d, J_{PC} = 2.0 Hz, CH_{Ar}), 130.2 (d, J_{PC} = 12.1 Hz, CH_{Ar}), 130.0 (d, J_{PC} = 50.3 Hz, C_{Ar}), 129.9 (d, J_{PC} = 11.1 Hz, CH_{Ar}), 128.9 (dd, J_{PC} = 15.6 and 88.0 Hz, C_{Ar}), 125.5 (d, J_{PC} = 85.5 Hz, C_{Ar}), 121.1 (q, J_{FC} = 320.9 Hz, CF_3), –7.2 (ddd, J_{PC} = 12.1 and 38.2 Hz, J_{RhC} = 19.1 Hz, CH_2); HRMS (ESI^+): 591.0514 calcd for $C_{32}H_{26}OP_2Rh^+$ $[M - CO - TfO]^+$, found, 591.0527; IR (CH_2Cl_2): 2024, 2082 cm^{-1}.

Synthesis of [L^NRh(COD)](BF_4) complex.

KHMDS (70 mg, 0.35 mmol) was added to a suspension of **L^NH.BF_4** (211 mg, 0.35 mmol) in THF (8 mL), the suspension rapidly turned into a clear yellow solution. The ^{31}P NMR analysis of the crude mixture shows the formation of **L^N** (δ_P = –1.2 and –13.7 ppm, J_{PP} = 13.0 Hz). The slight suspension was filtered through a PTFE filter, THF was removed under vacuum and the obtained yellow solid was dissolved in CH_2Cl_2 (6 mL) and $[Rh(COD)_2]_2(BF_4)$ (142 mg, 0.35 mmol) was added to the obtained solution. The reaction mixture is stirred 1h at room temperature then CH_2Cl_2 is evaporated and the obtained solid was stirred overnight with Et_2O (30 mL). Removal of the ether supernatant and drying under vacuum gave **[L^NRh(COD)](BF_4)** as a yellow orange solid (280 mg, 80%). $^{31}P\{^1H\}$ NMR (121.5 MHz, CD_2Cl_2, 25 °C): δ = 26.0 (dd, J_{RhP} = 159.0 Hz and J_{PP} = 25.0 Hz, P^{III}), 22.7 (d, J_{PP} = 25.0 Hz, PN); ^1H NMR (300 MHz, CD_2Cl_2, 25 °C): δ = 7.20–7.75 (m, 22H, CH_{Ar}), 7.11 (td, J_{PH} = 12.0 Hz, J_{HH} = 4.0 Hz, 1H, CH_{ArP2}), 6.96 (ddd, J_{HH} = 7.0 Hz, J_{PH} = 13.0 and 20.0 Hz, 4H, CH_{Ar}), 5.46 (br.s, 2H, CH_{COD}), 3.18 (dtd, J_{PH} = 20.0 Hz, J_{HH} = 6.5 and 2.0 Hz, 1H, C*H*(CH_3)$_2$), 3.00 (br.s, 2H, CH_{COD}), 1.60–2.00 (m, 8H, CH_{2COD}), 0.47 (d, J_{HH} = 6.5 Hz, 6H, CH(C*H*$_3$)$_2$); $^{13}C\{^1H\}$ NMR (75.0 MHz, CD_2Cl_2, 25 °C): δ = 138.0 (d, J_{PC} = 9.0 Hz, CH_{Ar}), 136.2 (d, J_{PC} = 106.0 Hz, C_{Ar}), 136.1 (*J* not measurable C_{Ar}), 135.6 (dd, J_{PC} = 13.5 and 10.0 Hz, CH_{Ar}), 135.0 (d, J_{PC} = 2.5 Hz, CH_{Ar}), 134.2 (d, J_{PC} = 6.0 Hz, C_{Ar}), 133.8 (d, J_{PC} = 9.5 Hz, CH_{Ar}), 133.3 (d, J_{PC} = 3.0 Hz, CH_{Ar}), 133.1 (s, CH_{Ar}), 133.0 (s, CH_{Ar}), 132.9 (dd, J_{PC} = 5.5 and 2.5 Hz, CH_{Ar}), 131.7 (d, J_{PC} = 10.0 Hz, CH_{Ar}), 131.2 (s, CH_{Ar}), 130.7 (dd, J_{PC} = 12.5 and 2.0 Hz, CH_{Ar}), 129.8 (d, J_{PC} = 13.5 Hz, CH_{Ph}), 129.4 (d, J_{PC} = 12.0 Hz, CH_{Ph}), 129.0 (d, J_{PC} = 10.0 Hz, CH_{Ph}), 122.0 (*J* not measurable, C_{Ph}), 107.1 (br.s, *J* not measurable, CH_{COD}), 50.6 (br.s, *J* not measurable, C*H*(CH_3)$_2$), 30.9 (s, CH_{2COD}), 28.0 (s, CH_{2COD}), 26.7 (s, br.s, *J* not measurable, CH(C*H*$_3$)$_2$), 25.4 (vt, J_{RhC} = J_{PC} = 9.0 Hz, CH_{2COD}). HRMS (ESI^+/Q-TOF): calcd 714.1913 for $C_{41}H_{43}NP_2Rh^+$ $[M]^+$, found: 714.1920. Elemental analysis for $C_{41}H_{43}BF_4NP_2Rh$.(0.4 CH_2Cl_2): calcd, C 59.52, H 5.28, N 1.68; found, C 59.46, H 5.18, N 1.85.

Synthesis of [L^NRh(CO)$_2$](BF$_4$) complex.

CO was bubbled into a CH_2Cl_2 (4 mL) solution of **[L^NRh(COD)](BF$_4$)** (58 mg, 0.06 mmol) during 3 minutes and stirring was continued for 1 h. The solvent was removed under vacuum, and the resulting solid was stirred with Et_2O (15 mL) during 1h. **[L^NRh(CO)$_2$](BF$_4$)** was isolated after removal of the ether supernatant and drying under vacuum as a red-brown solid (44 mg, 85 %). $^{31}P\{^1H\}$ NMR (121.5 MHz, CD_2Cl_2, 25 °C): δ = 13.7 (dd, J_{RhP} = 129.0 Hz and J_{PP} = 28.5 Hz, P^{III}), 28.7 (d, J_{PP} = 28.5 Hz, PN); ^1H NMR (CD_2Cl_2, 300 MHz) : δ = 7.82 (qd, J_{PH} = 8.5 Hz, J_{HH} = 8.0 and 1.0 Hz, 4H, CH_{Ar}), 7.72–7.60 (m, 8H, CH_{Ar}), 7.53 (ddd, J_{PH} = 13.5 and 2.0 Hz, J_{HH} = 8.0 Hz, 8H, CH_{Ar}), 7.45 (dd, J_{HH} = 7.5 Hz, J_{PH} = 9.0 Hz, 2H, CH_{Ar}), 7.40 (dd, J_{HH} = 7.5 Hz, J_{PH} = 9.0 Hz, 2H, CH_{Ar}), 3.34 (hept, J_{HH} = 6.5 Hz, J_{PH} not measurable, 1H, C*H*(CH_3)$_2$), 0.90 (d, J_{HH} = 6.5 Hz, 6H, CH(C*H*$_3$)$_2$); $^{13}C\{^1H\}$ NMR (CD_2Cl_2, 75 MHz) : δ = 183.9 (d, J_{RhC} = 64.5 Hz, J_{PC} not measured, CO), 181.7 (d, J_{RhC} = 61.5 Hz, J_{PC} not measured, CO), 138.2 (d, J_{PC} = 9.5 Hz, CH_{Ar}), 136.2 (dd, J_{PC} = 12.5 and 9.0 Hz, CH_{Ar}), 135.6 (d, J_{PC} = 4.0 Hz, C_{Ar}), 135.5 (d, J_{PC} = 3.0 Hz, CH_{Ar}), 135.3 (d, J_{PC} = 4.0 Hz, C_{Ar}), 134.8 (d, J_{PC} = 5.0 Hz, CH_{Ar}), 134.5 (dd, J_{PC} = 7.0 and 2.5 Hz, C_{ArP2}), 134.0 (d, J_{PC} = 8.5 Hz, CH_{Ph}), 133.8 (d, J_{PC} = 6.0 Hz, CH_{Ph}), 132.6 (d, J_{PC} = 2.5 Hz, CH_{Ar}), 132.3 (d, J_{PC} = 2.0 Hz, CH_{Ar}), 132.2 (s, CH_{Ar}), 132.1 (*J* not observed, CH_{Ar}), 130.2 (d, J_{PC} = 24.0 Hz, CH_{Ar}), 130.1 (s, CH_{Ar}), 129.8 (d, J_{PC} = 14.0 Hz, C_{Ar}), 129.5 (d, J_{PC} = 12.5 Hz, CH_{Ph}), 126.8 (d, J_{PC} = 101.5 Hz, C_{Ph}), 51.1 (d, J_{PC} = 1.0 Hz, *C*H(CH_3)$_2$), 27.7 (d, J_{PC} = 1.0 Hz, CH(*CH*$_3$)$_2$). HRMS (ESI^+/Q-TOF): 634.0931 calcd for $C_{34}H_{31}NOP_2Rh^+$ ([M-CO]$^+$), found: 634.0930. IR (CH_2Cl_2): 2084, 2018, 1987, 1437, 1204, 1172 cm^{-1}.

Synthesis of [L^NRh(CO)Cl] complex.

KHMDS (20 mg, 0.1 mmol) was added to a suspension of **L^NH.BF$_4$** (59 mg, 0.1 mmol) in THF (3 mL), the suspension rapidly turned into a clear yellow solution. The ^{31}P NMR analysis of the crude mixture shows the formation of **L^N** (δ_P = –1.2 and –13.7 ppm, J_{PP}= 13.0 Hz). The slight suspension was filtered through a PTFE filter, THF was removed under vacuum. A solution of [Rh(CO)$_2$Cl]$_2$ in CH_2Cl_2 (2 mL) was added to the obtained solid. The reaction mixture was stirred 30 min at room temperature and then CH_2Cl_2 was removed under vacuum. The obtained solid was washed with Et_2O (2x5 mL) and dried under vacuum to give **[L^NRh(CO)Cl]** as a yellow orange solid (34 mg, 49%). $^{31}P\{^1H\}$ NMR (CD_2Cl_2, 121.5 MHz): δ = 36.1 (dd, J_{RhP} = 180.5 Hz and J_{PP} = 26.5 Hz, P^{III}), 19.7 (d, J_{PP} = 26.5 Hz, PN); ^1H NMR (CD_2Cl_2, 300 MHz): δ = 7.76 (dd, J_{PH} = 12.0 Hz and J_{HH} = 7.5 Hz, 4H, CH_{Ph}), 7.68 (td, J_{PH} = 2.0 Hz and J_{HH} = 7.5 Hz, 2H, CH_{Ph}), 7.58–7.40 (m , 18H, CH_{Ar}), 7.34–7.31 (m , 2H, CH_{Ar}), 3.20 (hd, $J_{PH} \approx$ 13.0 Hz and J_{HH} = 6.5 Hz, 1H, C*H*(CH_3)$_2$), 0.94 (d, J_{HH} = 6.5 Hz, 6H, CH(C*H*$_3$)$_2$); $^{13}C\{^1H\}$ NMR

(CD_2Cl_2, 75 MHz): δ = 188.1 (d, J_{RhC} = 56.0 Hz, CO), 137.3 (dd, J_{PC} = 100.0 and 14.5 Hz, C_{Ar}), 137.1 (d, J_{PC} = 10.0 Hz, CH_{Ar}), 135.8 (dd, J_{PC} = 51.5 and 1.0 Hz Hz, C_{Ar}), 135.6 (d, J_{PC} = 8.5 Hz, C_{Ar}), 135.4 (d, J_{PC} = 6.5 Hz, CH_{Ar}), 134.9 (d, J_{PC} = 10.0 Hz, CH_{Ph}), 133.7 (dd, J_{PC} = 12.0 and 1.0 Hz, CH_{Ph}), 133.1 (d, J_{PC} = 3.0 Hz, CH_{Ar}), 132.5 (dd, J_{PC} = 2.5 and 6.0 Hz, CH_{Ar}), 130.7 (d, J_{PC} = 2.5 Hz, CH_{Ar}), 130.0 (dd, J_{PC} = 12.5 and 2.0 Hz, CH_{Ar}), 129.8 (d, J_{PC} = 100.0 Hz, C_{Ph}), 129.2 (d, J_{PC} = 12.5 Hz, CH_{Ph}),128.9 (d, J_{PC} = 10.5 Hz, CH_{Ph}), 51.2 (s, $CH(CH_3)_2$), 27.9 (d, J_{PC} = 8.5 Hz, $CH(CH_3)_2$). HRMS (ESI^+/Q-TOF): 634.0931 calcd for $[C_{34}H_{31}NOP_2Rh]^+$ [M-CO-Cl]$^+$, found: 634.0930. IR (CH_2Cl_2): 1972, 1435, 1174, 1109, 1096 cm^{-1}. Elemental analysis for $C_{34}H_{31}ClNOP_2Rh.(0.4\ CH_2Cl_2)$: calcd, C 58.70, H 4.55, N 1.99; found, C 58.57, H 4.39, N 2.07.

Single-Crystal X-ray Diffraction Analyses.

For **L^CH.OTf** and **[L^CRh(CO)$_2$](OTf)**, single crystals suitable for X-ray diffraction were coated with paratone oil and mounted onto the goniometer. The X-ray crystallographic data were obtained at 100K from a Rigaku XtaLAB Synergy diffractometer (Cu Kα radiation source) equipped with an Oxford Cryosystem. The structures have been solved using Superflip[29] and refined by means of least-squares procedures on F using the program CRYSTALS.[30] The scattering factors for all the atoms were used as listed in the International Tables for X-ray Crystallography.[31] Absorption correction was performed using a MULTISCAN procedure.[32] All non-hydrogen atoms were refined anisotropically. The H atoms were refined with riding constraints. For **L^N** Rh complexes, data were collected at 150 K on a Bruker Kappa APEX II (**[L^NRh(COD)](BF$_4$)** and **[L^NRh(CO)Cl]**) or a Stoe Stradivari (**[L^NRh(CO)$_2$](BF$_4$)**) diffractometer using a Mo-κ (λ = 0.71069Å) X-ray source and a graphite monochromator. The crystal structures were solved using Shelxt[33] or olex[34] and refined using Shelxl-97 or Shelxl-2014.[35] ORTEP drawings were made using ORTEP III[36] for Windows. Details of crystal data and structure refinements are summarized in Tables S1-2.

Molecular Modeling.

Molecular modeling was performed at density functional theory (DFT) level using consistently the Gaussian 16 code.[37] Geometry optimization was performed with the help of the B3LYP exchange correlation functional[38] and the LANLDZ basis set, including pseudopotential for heavy atoms (Rhodium). Vibrational frequencies have been obtained within the harmonic approximation from the hessian matrix, calculated at the same level of theroy as for the geometry optimization. Dichloromethane solvent was implicitly taken into account in all calculations by using the polarizable continuum model (PCM)[39] as implemented in Gaussian16. The oxidation potentials have been estimated considering the differences between the free

energy of the reduced, i.e. monocationic, and oxidized, i.e. dicationic, species at the respective equilibrium geometries. The same level of theory, i.e. B3LYP/LANL2DZ, has been used and free energy has been obtained by the harmonic vibrational frequencies considering the rigid rotor approximation, and further converted to electrochemical potentials using the Nernst law. To assess the effect of the basis set the NPA charges for the parent complexes have been calculated with a triple zeta basis set, namely LANL2TZ(f) for Rh and 6-311G* for the lighter atoms, showing no significant differences with those obtained at double-zeta level, and hence confirming our choice of the level of theory.

ASSOCIATED CONTENT

Supporting Information.

The Supporting Information is available free of charge on the ACS Publications website.

^{1}H, ^{31}P and ^{13}C NMR for all new compounds, solution IR spectra for **[L^{C}Rh(CO)$_2$](OTf)**, **[L^{N}Rh(CO)$_2$](BF$_4$)**, **[L^{N}Rh(CO)Cl]** and **[L^{N}Rh(CO)](BF$_4$)**, and additional crystallographic data for **L^{C}H.OTf**, **[L^{C}Rh(CO)$_2$](OTf)**, [**L^{N}Rh(COD)](BF$_4$)**, **[L^{N}Rh(CO)$_2$](BF$_4$)**, and **[L^{N}Rh(CO)Cl]**. DFT Optimized geometries of the different Rh(CO)$_2$ complexes.

AUTHOR INFORMATION

Corresponding Authors.

* E-mail for Y.C.: yves.canac@lcc-toulouse.fr

* E-mail for A.A.: audrey.auffrant@polytechnique.edu

* E-mail for A.M.: antonio.monari@u-paris.fr

ORCID

Yves Canac: 0000-0002-3747-554X

Audrey Auffrant: 0000-0001-6952-4775

Antonio Monari: 0000-0001-9464-1463

ACKNOWLEDGEMENTS

The authors thank the Centre National de la Recherche Scientifique (CNRS), Ecole polytechnique for financial support, Alix Saquet for electrochemistry experiments and Dr. S. Bourcier for mass spectrometry measurements. ANR is acknowledged for the funding of the LYMACATO project (ANR-21-CE07-0026-01), and the GDR phosphore for gathering the community of P-chemists in France. A.M. also thanks ANR and CGI (Commissariat à l'Investissement d'Avenir) for their financial support of this work through Labex SEAM

(Science and Engineering for Advanced Materials and devices), ANR 11 LABX 086 and ANR 11 IDEX 05 02. The support of the IdEx “Université Paris 2019” ANR-18-IDEX-0001 and of the Platform P3MB is gratefully acknowledged.

REFERENCES AND NOTES

(1) Michaelis, A.; Gimborn, H. V. Ueber das betaiï und cholin des triphenylphosphins. *Ber. Dtsch. Chem. Ges*. **1894**, *27*, 272−277.

(2) Staudinger, H.; Meyer, J. Über neue organische phosphorverbindungen III. Phosphinmethylenderivate und phosphinimine. *Helv. Chim. Acta* **1919**, *2*, 635–646.

(3) (a) Wittig, G.; Rieber, M. Über die metallierLarkeit von quaternären ammonium- und phosphonium-Salzen. *Liebigs Ann. Chem*. **1949**, *562*, 177–192. (b) Wittig, G.; Geissler, G. Zur reaktionsweise des pentaphenyl-phosphors und einiger Derivate. *Liebigs Ann. Chem*. **1953**, *580*, 44–57. (c) H. Wamhoff, G. Richardt, S. Stölben Iminophosphoranes: Versatile tools in heterocyclic synthesis. *Adv. Heterocycl. Chem*. **1995**, *64*, 159–249.

(4) (a) Lischka, H. Electronic structure and proton affinity of methylenephosphorane by ab initio methods including electron correlation. *J. Am. Chem. Soc*. **1977**, *99*, 353**–**360. (b) Gonbeau, D.; Pfister-Guillouzo, G.; Mazières, M. R.; Sanchez, M. La liaison phosphore–azote. Étude quantochimique de modèles neutres et ioniques H_3PNH, $H_3PNH_2^+$, $H_2PNH_3^+$, H_2PNH^- et $HPNH_2^-$. *Can. J. Chem.* **1985**, *63*, 3242**–**3248. (c) Molina, P.; Alajarin, M.; Leonardo, C. L.; Claramunt, R. M.; Foces-Foces, M. d. l. C.; Cano, F. H.; Catalan, J.; Paz, J. L. G. D.; Elguero, J. Experimental and theoretical study of the R_3P^+-X^- bond. Case of betaines derived from N-iminophosphoranes and alkyl isocyanates. *J. Am. Chem. Soc.* **1989**, *111*, 355–363. (d) Sudhakar, P. V.; Lammertsma, K. Nature of bonding in phosphazoylides. A comparative study of N_2H_4, NPH_4, and P_2H_4. *J. Am. Chem. Soc.* **1991**, *113*, 1899**–**1906.

(5) (a) Reed, A. E.; von Ragué Schleyer, P. Chemical bonding in hypervalent molecules. The dominance of ionic bonding and negative hyperconjugation over d-orbital participation. *J. Am. Chem. Soc.* **1990**, *112*, 1434−1445. (b) Gilheany, D. G. No d orbitals but Walsh diagrams and maybe banana bonds: chemical bonding in phosphines, phosphine oxides, and phosphonium ylides. *Chem. Rev.* **1994**, *94*, 1339−1374. (c) Yufit, D. S.; Howard, J. A. K.; Davidson, M. G. Bonding in phosphorus ylides: topological analysis of experimental charge density distribution in triphenylphosphonium benzylide. *J. Chem. Soc., Perkin Trans. 2* **2000**, 249−253. (d) Chesnut, D. B. An electron localization function investigation of bonding in some simple four-coordinate nitrogen and phosphorus compounds. *Heteroatom Chem.* **2000**, *11*, 341−352. (e) Kocher, N.; Leusser, D.; Murso, A.; Stalke, D. Metal coordination to the formal P=N bond of an iminophosphorane and charge-density evidence against hypervalent phosphorus(v). *Chem.*

Eur. J. **2004**, *10*, 3622−3631. (f) Alabugin, I. V.; Dos Passos Gomes, G.; Abdo, G, M. A. Hyperconjugaison. *WIREs Comput Mol Sci*. **2019**;*9*:e1389.
(6) Koketsu, J.; Ninomiya, Y.; Suzuki, Y.; Koga, N. Theoretical study on the structures of iminopnictoranes and their reactions with formaldehyde. *Inorg. Chem.* **1997**, *36*, 694−702.
(7) Calhorda, M. J.; Krapp A.; Frenking, G. A new look at the ylidic bond in phosphorus ylides and related compounds: Energy decomposition analysis combined with a domain-averaged Fermi hole analysis. *J. Phys. Chem. A*, **2007**, *111*, 2859–2869, and references cited herein.
(8) (a) Schmidbaur, H. Phosphorus ylides in the coordination sphere of transition metals: an inventory. *Angew. Chem. Int. Ed. Engl.* **1983**, *22*, 907–927. (b) Kaska, W. C.; Ostoja Starzewski, K. A, Transition metal complexes with ylides in: *Ylides and Imines of Phosphorus*; Johnson, A. W., Eds, John Wiley & Sons: New York, **1993**, chapter 14. (c) Kolodiazhnyi, O. I. C-element-substituted phosphorus ylides. *Tetrahedron* **1996**, *52*, 1855–1929. (d) Vicente, J. Chicote, M. T. The 'acac method' for the synthesis and coordination of organometallic compounds: synthesis of gold complexes. *Coord. Chem. Rev*. **1999**, *193-195*, 1143–1161. (e) Falvello, L. R.; Ginés, J. C.; Carbó, J. J.; Lledós, A.; Navarro, R.; Soler, T.; Urriolabeitia, E. P. Palladium complexes of a phosphorus ylide with two stabilizing groups: synthesis, structure, and DFT study of the bonding modes. *Inorg. Chem.* **2006**, *45*, 6803–6815. (f) Urriolabeitia, E. P. sp^3-hybridized neutral η^1-carbon ligands. *Top. Organomet. Chem.* Chauvin, R.; Canac, Y. Eds, Springer, **2010**, *30*, 15–48. (g) Valyaev, D. A.; Canac, Y. Carbenes and phosphonium ylides: a fruitful association in coordination chemistry. *Dalton Trans*. **2021**, *50*, 16434−16442.
(9) (a) Johnson, A. W. Iminophosphoranes and related compounds in: *Ylides and Imines of Phosphorus*; Johnson, A. W., Eds, John Wiley & Sons: New York, **1993**, chapter 13. (b) Cantat, T.; Mezailles, N.; Auffrant, A.; Le Floch, P. Bis-phosphorus stabilized carbene complexes. *Dalton Trans.* **2008**, 1957−1972. (c) Harder, S. Geminal dianions stabilized by phosphonium substituents. *Coord. Chem. Rev.* **2011**, *255*, 1252−1267. (d) Johnson, K. R. D.; Hayes, P. G. Cyclometalative C-H bond activation in rare earth and actinide metal complexes. *Chem. Soc. Rev.* **2013**, *42*, 1947−1960. (e) Mustieles Marín, I.; Auffrant, A. Phosphasalen vs. Salen Ligands: What does the phosphorus change? *Eur. J. Inorg. Chem.* **2018**, *2018*, 1634–1644. (f) Fustier-Boutignon, M.; Nebra, N.; Mézailles, N. Geminal dianions stabilized by main group elements. *Chem. Rev*. **2019**, 119, 8555−8700. (g) García-Garrido, S. E.; Presa Soto, A.; García-Álvarez, J. Iminophosphoranes (R_3PNR'): From terminal to multidentate ligands in organometallic chemistry. in *Advances in Organometallic Chemistry*, Pérez, P. J., Ed., Academic Press, **2022**, 105−168.
(10) *For phosphonium ylides, see*: (a) Berthe, J.; Garcia, J. M.; Ocando, E.; Kato, T.; Saffon-Merceron, N.; De Cozar, A.; Cossio, F. P.; Baceiredo, A. Synthesis and reactivity of a

phosphine-stabilized monogermanium analogue of alkynes. *J. Am. Chem. Soc*. **2011**, *133*, 15930–15933. (b) Alvarado-Beltran, I.; Baceiredo, A.; Saffon-Merceron N.; Branchadell, V.; Kato, T. Cyclic amino(ylide) silylene: A stable heterocyclic silylene with strong electron-donating character. *Angew. Chem. Int. Ed*. **2016**, *55*, 16141–16144. (c) Scherpf, T.; Feichtner, K. S.; Gessner, V. H. Using ylide functionalization to stabilize boron cations. *Angew. Chem. Int. Ed*. **2017**, *56*, 3275–3279. (d) Mohapatra, C.; Scharf, L.; Scherpf, T.; Mallick, B.; Feichtner, K-S.; Schwarz, C.; Gessner, V. H. Isolation of a diylide-stabilized stannylene and germylene: enhanced donor strength coplanar lone pair alignment. *Angew. Chem. Int. Ed*. **2019**, *58*, 7459–7463. *For iminophosphoranes, see*: (e) Ong, C. M.; McKarns, P.; Stephan, D. W. Neutral and cationic group 13 phosphinimine and phosphinimide complexes. *Organometallics* **1999**, *18*, 4197–4204. (f) Smith, D. A.; Batsanov, A. S.; Miqueu, K.; Sotiropoulos, J.-M.; Apperley, D. C.; Howard, J. A. K.; Dyer, P. W. A truly multifunctional heterocycle: iminophosphorane, N,P chelate, and dihydropyridine. *Angew. Chem. Int. Ed.* **2008**, *47*, 8674–8677. (g) Xiong, Y.; Yao, S.; Inoue, S.; Berkefeld, A.; Driess, M. Taming the germyliumylidene $[ClGe:]^+$ and germathionium $[ClGe{=}S]^+$ ions by donor–acceptor stabilization using 1,8-bis(tributylphosphazenyl)naphthalene. *Chem. Commun.* **2012**, *48*, 12198–12200. (h) Thirumoorthi, R.; Chivers, T.; Gendy, C.; Vargas-Baca, I. CH–NH Tautomerism in the products of the reactions of the methanide $[HC(PPh_2NSiMe_3)_2]-$ with pnictogen and tellurium iodides. *Organometallics* **2013**, *32*, 5360–5373. (i) Kögel, J. F.; Xie, X.; Baal, E.; Gesevičius, D.; Oelkers, B.; Kovačević, B.; Sundermeyer, J. Superbasic Alkyl-substituted bisphosphazene proton sponges: synthesis, structural features, thermodynamic and kinetic basicity, nucleophilicity and coordination chemistry. *Chem. Eur. J.* **2014**, *20*, 7670–7685. (j) Ochiai, T.; Franz, D.; Inoue, S. Applications of N-heterocyclic imines in main group chemistry. *Chem. Soc. Rev*. **2016**, *45*, 6327–6344. (k) Zhang, J.; Ge, S.; Zhao, J.; Ulhaq, I.; Ferguson, M. J.; McDonald, R.; Maa, G.; Cavell, R. G. Synthesis and structures of bis(iminophosphorano)methanide chelate complexes with zinc and group 13. *Polyhedron* **2019**, *159*, 167–175.

(11) *For phosphonium ylides, see*: (a) Canac, Y.; Lepetit, C.; Chauvin R. Neutral η^1-carbon ligands: Beyond carbon monoxide. *Top. Organomet. Chem.* Chauvin, R.; Canac, Y. Eds, Springer, **2010**, *30*, 1–12. (b) Serrano, E.; Soler, T.; Urriolabeitia, E. P. Regioselective C-H bond activation of asymmetric bis(ylide)s promoted by Pd. *Eur. J. Inorg. Chem*. **2017**, 2220–2230. (c) Taakili, R.; Lepetit, C.; Duhayon, C.; Valyaev, D. A.; Lugan, N.; Canac, Y. Palladium(II) pincer complexes of a *C,C,C*-NHC, diphosphonium bis(ylide) ligand. *Dalton Trans*. **2019**, *48*, 1709−1721. (d) Taakili, R.; Barthes, C.; Lepetit, C.; Duhayon, C.; Valyaev, D. A.; Canac, Y. Direct access to palladium(II) complexes based on anionic *C,C,C*-phosphonium ylide core pincer ligand. *Inorg. Chem.* **2021**, *60*, 12116−12128. (e) El Kadiri, M.;

Chihab, A.; Taakili, R.; Duhayon, C.; Valyaev, D. A.; Canac, Y. Diverse *C*-coordination modes of NHC-tricyclohexylphosphonium ylide ligands in palladium(II) complexes. *Organometallics* **2022**, *41*, 456–466. *For iminophosphoranes*, see: (f) Al-Benna, S.; Sarsfield, M. J.; Thornton-Pett, M.; Ormsby, D. L.; Maddox, P. J.; Bres, P.; Bochmann, M. Sterically hindered iminophosphorane complexes of vanadium, iron, cobalt and nickel: a synthetic, structural and catalytic study. *J. Chem. Soc. Dalton Trans.* **2000**, 4247–4257. (g) Bielsa, R.; Navarro, R.; Soler, T.; Urriolabeitia, E. P. Orthopalladation of iminophosphoranes: synthesis, structure and study of stability. *Dalton Trans.* **2008**, 1203–1214. (h) Cheisson, T., Auffrant, A. Versatile coordination chemistry of a bis(methyliminophosphoranyl)pyridine ligand on copper centres. *Dalton Trans.* **2014**, *43*, 13399–13409. (i) Suzuki, T.; Masuda, H.; Fryzuk, M. D. Variable coordination geometries via an amine-tethered-enamidophosphinimine ligand on cobalt. *Dalton Trans.* **2017**, *46*, 6612–6622. (j) Azouzi, K.; Duhayon, C.; Benaissa, I.; Lugan, N.; Canac, Y.; Bastin, S.; César, V. Bidentate iminophosphorane-NHC ligand derived from the imidazo[1,5-*a*]pyridin-3-ylidene scaffold. *Organometallics*, **2018**, *37*, 4726–4735. (k) Cheisson, T.; Ricard, L.; Heinemann, F. W.; Meyer, K.; Auffrant, A.; Nocton, G. Synthesis and reactivity of low-valent f-element iodide complexes with neutral iminophosphorane ligands. *Inorg. Chem.* **2018**, *57*, 9230–9240. (l) MacNeil, C. S.; Hayes, P. G. An H-substituted rhodium silylene. *Chem. Eur. J.* **2019**, *25*, 8203–8207. (m) Normand, A. T.; Sosa Carrizo, E. D.; Magnoux, C.; Lobato, E.; Cattey, H.; Richard, P.; Brandes, S.; Devillers, C. H.; Romieu, A.; Le Gendre, P.; Fleurat-Lessard, P. Reappraising Schmidpeter's bis(iminophosphoranyl)phosphides: coordination to transition metals and bonding analysis. *Chem. Science* **2021**, *12*, 253–269. (n) Winslow, C.; Lee, H. B.; Field, M. J.; Teat, S. J.; Rittle, J. Structure and reactivity of a high-spin, nonheme iron(III)-superoxo complex supported by phosphinimide ligands. *J. Am. Chem. Soc.* **2021**, *143*, 13686–13693. (o) Tannoux, T.; Auffrant, A. Complexes featuring tridentate iminophosphorane ligands: Synthesis, reactivity, and catalysis. *Coord. Chem. Rev*. **2023**, *474*, 214845.

(12) Hopkinson, M. N.; Richter, C.; Schedler, M.; Glorius, F. An overview of N-Heterocyclic carbenes. *Nature* **2014**, *510*, 485–496.

(13) (a) Gao, Y.; Pink, M.; Smith, J. M. Iron(II) complexes of an anionic bis(ylide)diphenylborate ligand. *Inorg. Chem.* **2020**, *59*, 17303−17309, and references cited herein. (b) Shi, Y.; Pan, B. W.; Yu, J. S.; Zhou, Y.; Zhou, J. Recent advances in applying carbonyl-stabilized phosphorus ylides for catalysis. *Chem. Cat. Chem*. **2021**, *13*, 129−139.

(14) Grey, R. A.; Anderson, L. R. Preparation, characterization, and catalytic reactions of cyclooctadiene(dimethylphosphonium bis (methylide)) rhodium (I) and its carbonyl derivatives. *Inorg. Chem*. **1977**, *16*, 3187−3190.

(15) Taakili, R.; Barthes, C.; Goëffon, A.; Lepetit, C.; Duhayon, C.; Valyaev, D. A.; Canac, Y. NHC core phosphonium ylide-based palladium(II) pincer complexes: The second ylide extremity makes the difference. *Inorg. Chem*. **2020**, *59*, 7082–7096.
(16) See for examples: (a) Spencer, L. P.; Altwer, R.; Pingrong Wei, L. G.; Gauld, J.; Stephan, D. W. Pyridine - and imidazole - phosphinimine bidentate ligand complexes: considerations for ethylene oligomerization catalysts. *Organometallics* **2003**, *22*, 3841–3854. (b) Buchard, A.; Komly, B.; Auffrant, A.; Le Goff, X. F.; Le Floch, P. A mixed phosphine-iminophosphorane tetradentate ligand: Synthesis, coordination to group 10 metal centers, and use as catalyst in Suzuki-Miyaura coupling. *Organometallics* **2008**, *27*, 4380−4385. (c) Wheaton, C. A.; Hayes, P. G., Exploring the versatility of a bis(phosphinimine) pincer ligand: effect of sterics on structure and lactide polymerization activity of cationic zinc complexes. *Catal. Sc. & Technol.* **2012**, *2*, 125–138. (d) Zhang, X. Q.; Wang, Z. X. Cross-coupling of aryltrimethylammonium iodides with arylzinc reagents catalyzed by amido pincer nickel complexes. *J. Org. Chem.* **2012**, *77*, 3658–3663. (e) Martinez-Arripe, E.; Jean-Baptiste-dit-Dominique, F.; Auffrant, A.; Le Goff, X. F.; Thuilliez, J.; Nief, F. Synthesis and characterization of bidentate rare-earth iminophosphorane o-aryl complexes and their behavior as catalysts for the polymerization of 1,3-Butadiene. *Organometallics* **2012**, *31*, 4854−4861. (f) Rong, W. F.; Liu, D. T.; Zuo, H. P.; Pan, Y. P.; Jian, Z. B.; Li, S. H.; Cui, D. M. Rare-earth-metal complexes bearing phosphazene ancillary ligands: structures and catalysis toward highly trans-1,4-Selective (co)polymerizations of conjugated dienes. *Organometallics* **2013**, *32*, 1166–1175. (g) García-Álvarez, J.; García-Garrido, S. E.; Cadierno, V. Iminophosphorane–phosphines: versatile ligands for homogeneous catalysis. *J. Organomet. Chem.* **2014**, *751*, 792–808. (h) Cheisson, T.; Cao, T. P. A.; Le Goff, X. F.; Auffrant, A. Nickel complexes featuring iminophosphorane−phenoxide ligands for catalytic ethylene dimerization. *Organometallics* **2014**, *33*, 6193–6199. (i) Mou, Z. H.; Liu, B.; Liu, X. L.; Xie, H. Y.; Rong, W. F.; Li, L.; Li, S. H.; Cui, D. M. Efficient and heteroselective heteroscorpionate rare-earth-metal zwitterionic initiators for ROP of rac-lactide: role of sigma-ligand. *Macromolecules* **2014**, *47*, 2233–2241. (j) Liu, N.; Liu, D. D.; Liu, B.; Zhang, H.; Cui, D. M. Stereoselective polymerization of rac-lactide catalyzed by zwitterionic calcium complexes. *Polym. Chem.* **2021**, *12*, 1518–1525.
(17) (a) Canac, Y.; Lepetit, C.; Abdalilah, M.; Duhayon, C.; Chauvin, R. Diaminocarbene and phosphonium ylide ligands: a systematic comparison of their donor character. *J. Am. Chem. Soc*. **2008**, *130*, 8406–8413. (b) Canac, Y.; Lepetit, C. Classification of the electronic properties of chelating ligands in *cis*-[LL'Rh(CO)$_2$] complexes. *Inorg. Chem*. **2017**, *56*, 667−675.
(18) Viau, L.; Lepetit, C.; Commenges, G. ; Chauvin, R. Chiral phosphine-phosphonium ylide rhodium complexes. *Organometallics* **2001**, *20*, 808−810.

(19) CCDC numbers for compounds **L^CH.OTf**, **[L^CRh(CO)$_2$](OTf)**, **[L^NRh(COD)](BF$_4$)**, **[L^NRh(CO)$_2$](BF$_4$)**, and **[L^NRh(CO)Cl]**: 2190071-2190075. These data can be obtained free of charge from the Cambridge Crystallographic Data Centre via www.ccdc.cam.ac.uk/data_request/cif.

(20) Zurawinski, R.; Donnadieu, B.; Mikolajczyk, M.; Chauvin R. Chiral phosphino(sulfinylmethyl)triarylphosphonium ylide ligands: Rhodium complexes and catalytic properties. *Organometallics* **2003**, *22*, 4810−4817.

(21) Buchard, A.; Auffrant, A.; Klemps, C.; Vu-Do, L.; Boubekeur, L.; Le Goff, X. F.; Le Floch, P. Highly efficient P-N nickel(II) complexes for the dimerisation of ethylene. *Chem. Commun.* **2007**, 1502−1504.

(22) Imhoff, P.; Vanasselt, R.; Elsevier, C. J.; Zoutberg, M. C.; Stam, C. H. Reactions of bis(iminophosphoranyl)methanes with chloro-bridged rhodium or iridium dimers giving complexes in which the ligand is coordinated either as a σ-N,σ-N' or as a σ-N,σ-C chelate. X-ray crystal structure of the σ-N,σ-N' Rh(I) complex [Rh{(4-CH_3-C_6H_4-N=PPh_2)CH_2}(COD)]PF_6. *Inorg. Chim. Acta* **1991**, *184*, 73−87.

(23) MacNeil, C. S.; Glynn, K. E.; Hayes, P. G. Facile activation and deoxygenative metathesis of CO. *Organometallics* **2018**, *37*, 3248−3252.

(24) For rare examples of 3-coordinate Rh(I) monocarbonyl complexes, see: (a) Deraniyagala, S. P.; Grundy, K. R. Synthesis of [Rh_2(μ-OR)$(CO)_2$(μ-$PPh_2CH_2PPh_2$)$_2$]ClO_4 (R = H, CH_3, C_2H_5) and their use as synthetic precursors to other A-frame complexes. *Inorg. Chem*. **1985**, *24*, 50−56. (b) Lavallo, V.; Canac, Y.; Dehope, A.; Donnadieu, B.; Bertrand, G. A rigid cyclic (alkyl)(amino)carbene ligand leads to isolation of low-coordinate transition metal complexes. *Angew. Chem. Int. Ed.* **2005**, *44*, 7236−7239.

(25) CCDC numbers for iminophosphorane Rh$(CO)_2$ complexes: 285955, 676924, 732170, 732171, 81488, 1822710, 1822713, 1822715.

(26) Those parameters are comparable to those measured for Rh$(CO)_2$ fragment supported by LX-type *N,N*-ligand within a porphyrin, see: Tanaka, T., Aratani, N.; Osuka, A. Aromatic-to-antiaromatic switching in triply linked porphyrin bis(rhodium(I)) hexaphyrin hybrids. *Chem. Asian J*. **2012**, *7*, 889–893. They are also similar to LRh$(CO)_2$Cl where L is a carbene-type ligand, see: (a) Dyker, C. A., Lavallo, V., Donnadieu, B.; Bertrand, G. Synthesis of an extremely bent acyclic allene (A "Carbodicarbene"): a strong donor ligand. *Angew. Chem. Int. Ed.* **2008**, *47*, 3206–3209. (b) Tennyson, A. G., Ono, R. J., Hudnall, T. W., Khramov, D. M., Er, J. A. V., Kamplain, J. W., Lynch, V. M., Sessler, J. L.; Bielawski, C. W. Quinobis(imidazolylidene): synthesis and study of an electron-configurable bis(N-heterocyclic carbene) and its bimetallic complexes. *Chem. Eur. J*. **2010**, *16*, 304–315. (c) Nakafuji, S.-Y.,

Kobayashi, J.; Kawashima, T. Generation and Coordinating properties of a carbene bearing a phosphorus ylide: an intensely electron-donating ligand. *Angew. Chem. Int. Ed*. **2008**, *47*, 1141−1144.

(27) Law, D. J.; Bigam, G.; Cavell, R. G. Preparation and properties of rhodium(I) and iridium(I) diolefin complexes of heterodifunctional phosphorus-imine chelating ligands and a related iminophosphine. ^{103}Rh NMR parameters of the rhodium complexes obtained via indirect two-dimensional ^{31}P, ^{103}Rh {^{1}H) NMR spectroscopy. *Can. J. Chem.* **1995**, *73*, 635−642.

(28) Reed, R. W.; Santarsiero, B.; Cavell, R. G. Selective azide oxidation of 1,2-bis(diphenylphosphino)benzene and related ethylenebis(phosphines) to asymmetric multifunctional phosphorus ligands and formation of rhodium(I) complexes of these ligands. Structural characterization of the prototypical ligand 1-(((trimethylsilyl)imino)diphenyl phosphorano)-2-(diphenylphosphino)benzene and its rhodium(I) complex: 1-$Ph_2P{=}N(SiMe_3)C_6H_4$-2-$(Ph_2P)Rh(CO)Cl$. *Inorg. Chem.* **1996**, *35*, 4292−4300.

(29) Palatinus, L.; Chapuis, G. Superflip – a computer program for the solution of crystal structures by charge flipping in arbitrary dimensions. *J. Appl. Cryst*. **2007**, *40*, 786−790.

(30) Betteridge, P. W.; Carruthers, J. R.; Cooper, R. I.; Prout, K.; Watkin, D. J. CRYSTALS version 12: software for guided crystal structure analysis. *J. Appl. Cryst.* **2003**, *36*, 1487.

(31) Sheldrick, G. M. A short history of SHELX. *Acta Cryst*. **2008**, *A64*, 112−122.

(32) Blessing, R. H. An empirical correction for absorption anisotropy. *Acta Cryst*. **1995**, *A51*, 33−38.

(33) Sheldrick, G. SHELXT - Integrated space-group and crystal-structure determination. *Acta Cryst. A* **2015**, *71,* 3–8.

(34) Dolomanov, O. V.; Bourhis, L. J.; Gildea, R. J.; Howard, J. A. K. Puschmann, H. OLEX2: a complete structure solution, refinement and analysis program. *J. Appl. Crystallogr.* **2009**, *42,* 339–341.

(35) Sheldrick, G. Crystal structure refinement with SHELXL. *Acta Cryst. C* **2015**, *71,* 3–8.

(36) Farrugia, L. J. *ORTEP-3 program*, Department of Chemistry, University of Glasgow: 2001.

(37) Gaussian 16 rev. A01 Frisch, M. J. Trucks, G. W. Schlegel, H. B. Scuseria, G. E. Robb, M. A. Cheeseman, J. R. Scalmani, G. Barone, V. Petersson, G. A. Nakatsuji, H. Li, X. Caricato, M. Marenich, A. V. Bloino, J. Janesko, B. G. Gomperts, R. Mennucci, B. Hratchian, H. P. Gaussian, Inc., Wallingford CT, 2016.

(38) Becke, A. *J. Chem. Phys.* **1993**, *98,* 5648–5652.

(39) Mennucci, B. *Wiley Inter. Rev*. **2012**, *2*, 386–404.

Table of Contents and Text

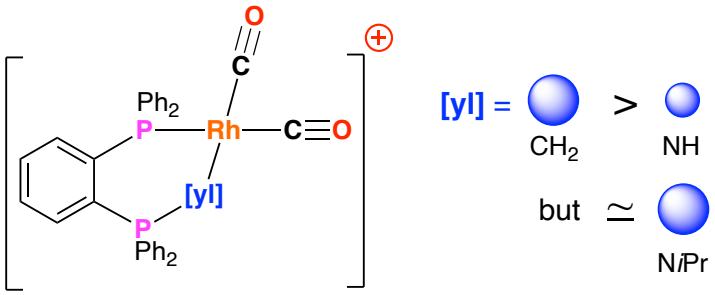

With an isopropyl substituent on N atom, the iminophosphorane can compete with the phosphonium ylide in terms of electron-donation in cationic *cis*-[phosphine-ylide $Rh^{I}(CO)_2$] complexes.